

## **FINAL REPORT**

# **DIPLOMA OF THE ROYAL MICROSCOPICAL SOCIETY**

**Peter Gabriel Pitrone**

**Building a Selective Plane Illumination Microscope System  
on a Limited Budget**

**June 15<sup>th</sup> 2014**



Administered by the Education and Outreach Committee of the Royal Microscopical Society on behalf of the Trustees of the Society.

Correspondence on all matters relating to the Diploma should be addressed to –

The Honorary Secretary for Education and Outreach, The Royal Microscopical Society, 37/38 St Clements Street, Oxford, OX2 0LY, UK t: +44 (0) 1865 254760 e: [diploma@rms.org.uk](mailto:diploma@rms.org.uk)

## SYNOPSIS

This dissertation is written to describe in a practical fashion how one can build, align, and use an open access light sheet microscope on a limited budget. The experience and feedback that has been implemented into the design of the light sheet microscope has been gained while working as a technical assistant for Dr. Pavel Tomancak at the Max Planck Institute of Molecular Cell Biology and Genetics (MPI-CBG) in Dresden Germany.

The Introduction and Aims section will cover the principles behind Light Sheet Fluorescence Microscopy (LSFM). There are two major designs for light sheet microscopy. I will describe how these different designs of light sheet microscopes work, explain the rationale for selecting the design adopted for this dissertation, and clarify what it is that we wanted to achieve with this project; both in regards to the biological research that our lab conducts, and in making the plans for the microscope freely available to the scientific community and the world.

In the Materials and Methods section detailed descriptions of the component assemblies, their relation to one another, and their alignment are given along with the reasons for their use will be discussed. Everyday use of the microscope in terms of sample preparation, operation of the microscope, and processing of the data is also introduced. The open access software programs and plugins associated with the hardware design are briefly explained in detail.

The Results section will cover practical testing of the system's stability and ability to produce meaningful, biologically relevant, and trustworthy datasets. The resolving power of the microscope depends both on the thickness of the light sheet, as well as the optical parameters of the detection objective. Protocols are described that enable the thickness of the light sheet to be measured, as well as measuring the Point Spread Function (PSF) of the detection lens. Besides the reliability of the optics of the microscope, it is crucial that the mechanical hardware components act precisely within understood tolerances. Imaging results of tissues and organs will also be presented.

The Discussion and Conclusion section concludes this report with a discussion of the areas in which the system can be made useful, where it is being used and by whom, along with our visions of where we can see it in the future.

## COMMONLY USED ABBREVIATIONS

### Micro-Imaging modality related abbreviations:

Light Sheet Fluorescence Microscopy	LSFM
Orthogonal-Plane Fluorescence Optical Sectioning	OPFOS
Selective Plane Illumination Microscopy	SPIM
Digitally Scanned Light sheet Microscopy	DSLM
Optical Projection Tomography	OPT
Laser Scanning Confocal Microscopy	LSCM

### Objective lens related abbreviations:

Numerical Aperture (of the objective)	NA
Back focal plane (of the objective)	BFP
Point Spread Function (of the objective)	PSF
Working Distance (of the objective)	WD

### Mathematics related abbreviations:

Full Width at Half Maxima	FWHM
---------------------------	------

### Society and institution related abbreviations:

Royal Microscopical Society	RMS
Max Planck Institute for Molecular Cell Biology and Genetics	MPI-CBG
Laboratory for Computational and Optical Instrumentation	LOCI

### Computer related abbreviations:

Fiji Is Just ImageJ	Fiji
Computer Aided Design	CAD

## LIST OF FIGURES AND TABLES

- Figure 1:** Solidworks rendering of the OpenSPIM system  
**Figure 2:** Sample Chamber assembly  
**Figure 3:** Water-dipping microscopy objectives  
**Figure 4:** Sample Positioning system  
**Figure 5:** Infinity space tube and optical filters  
**Figure 6:** Multiple magnification changer wheel (optional)  
**Figure 7:** Laser heat sink  
**Figure 8:** Kinematic mount assembly  
**Figure 9:** Spherical lens assembly  
**Figure 10:** Vertical slit assembly  
**Figure 11:** Cylindrical lens assembly  
**Figure 12:** Gimbal mount assembly  
**Figure 13:** Iris assembly (optional)  
**Figure 14:** Laser on heat sink in its position on the board  
**Figure 15:** Position of beam steering mirrors on the rail system  
**Figure 16:** Position of conjugate plane mirror on the rail system  
**Figure 17:** Position of beam expanding telescope on the rail system  
**Figure 18:** Position of cylindrical lens mount on the rail system  
**Figure 19:** Position of adjustable vertical slit on the rail system  
**Figure 20:** Position of conjugate plane telescope on the rail system  
**Figure 21:** Light sheet alignment and the function of the manual knobs  
**Figure 22:** Sample preparation mounting  
**Figure 23:** The main window of Image/Fiji  
**Figure 24:** The main window of  $\mu$ Manager  
**Figure 25:** Stage Control tab window  
**Figure 26:** The bottom portion of the Acquisition tab window  
**Figure 27:** The Position List sub-tab portion of the acquisition window  
**Figure 28:** The Video sub-tab portion of the acquisition window  
**Figure 29:** A graphical representation of the light sheet  
**Figure 30:** An image of the microscopy grid test sample  
**Figure 31:** The Set Scale window  
**Figure 32:** The plot profile window  
**Figure 33:** The Plot Values window  
**Figure 34:** Crop selection on a zoomed in Z-stack of a *Tribolium* embryo  
**Figure 35:** A plane by plane replay of the cropped bead through the Z-axis  
**Figure 36:** TransformJ window  
**Figure 37:** Crop selection on a zoomed in Y-stack of a *Tribolium* embryo  
**Figure 38:** A plane by plane replay of the cropped bead through the Y-axis  
**Figure 39:** Still frames of a beating heart  
**Figure 40:** Movie of a beating heart  
**Figure 41:** Image of a 2 days old zebrafish larva  
**Figure 42:** Movie of a stitched zebrafish larva  
**Figure 43:** Difference between fused and deconvolved datasets  
**Figure 44:** 3D rendering Drosophila embryos  
**Figure 45:** 3D movie rendering of Drosophila embryogenesis  
**Figure 46:** Multi-view time-lapse of the expression pattern of CSP  
**Figure 47:** Movie of drosophila embryos expressing CSP  
**Figure 48:** Conceptual design of a four system OpenSPIM farm  
**Figure 49:** Peter Gabriel Pitron teaching concepts of light sheet microscopy  
**Figure 50:** Image of OpenSPIM in a carry-on luggage container  
**Figure 51:** Image of Carsten Wolff's OpenSPIM system.

**Table 1:** Pixel sizes of images at different magnifications

**Table 2:** Differences between beam diameter and light sheet thickness

**Table 3:** Differences in speeds when Lase Full Stack

## CONTENT

1	Introduction and aims.....	6
1.1	Introduction to Light Sheet Fluorescence Microscopy.....	8
2	Materials and methods .....	12
2.1	Components of the microscope .....	12
2.2	Description of assembly steps .....	22
2.3	Light sheet alignment.....	26
2.4	Sample preparation .....	27
2.5	Operation of the microscope.....	28
2.6	Processing of multi-view data .....	33
3	Results.....	34
3.1	Light sheet characteristics .....	34
3.2	Measuring the Point Spread Function of the objective .....	37
3.3	Speed benchmarks.....	38
3.4	Imaging results.....	40
4	Discussion and conclusion.....	45
4.1	Areas where OpenSPIM can be useful.....	45
4.2	Other OpenSPIM systems being built.....	47
4.3	What does the future hold? .....	48
5	Appendix .....	50
5.1	List of references .....	50
5.2	List of website links .....	50
5.3	Acknowledgements .....	51

## I INTRODUCTION AND AIMS

Ever since the birth of the microscope at the end of the 16<sup>th</sup> century, microscopes have utilized first transmitted-light and then reflected-light illumination to view thin or translucent specimens and then thick/opaque samples. In transmitted-light, the illuminating and imaging rays are arranged along one axis, this being the simplest design to implement. Reflected-light microscope ray paths generally have the illumination shining down from one side above the specimen, or else it is shone sideways on and reflected onto the specimen by means of a mirror.

The phenomenon of fluorescence was named by Sir George Stokes in 1852, and first observed in microscopy by August Köhler at the turn of the 20<sup>th</sup> century in 1904. The early fluorescence microscopes were based on the transmitted-light design, and it wasn't until 1967 that JS Ploem developed the reflected-light illuminator for fluorescence microscopy that is universally used these days (Rusk N, 2009). There were good reasons for this:

- Alignment on-axis of a darkfield condenser is required while using a transmitted-light configuration. This can be done away with on an epi-fluorescence microscope where the objective acts as its own condenser
- A transmitted-light configuration necessarily relies upon very good blocking filters to prevent the harmful short wavelength excitation illumination reaching the eye and (which also reduces image contrast) the camera or electronic detector
- With a transmitted-light configuration, image brightness is proportional to the square of the (detection) objective numerical aperture (N.A.). In the epi-illumination configuration, image brightness is yet again squared, since the objective acts as its own condenser

The first use of illumination orthogonal to the objective was by Henry Siedentopf & Richard Zsigmondy while investigating colloids at the Carl Zeiss works in Jena (Siedentopf & Zsigmondy, 1903; Mappes et al 2012). At the beginning of the 20<sup>th</sup> century no sufficiently powerful darkfield condenser was available, nor were lasers known. To get around the first problem they shone a sheet of light side-on onto the sample. Because laser illumination wasn't invented until half a century later, carbon-arc burners were used. The first relevant use of a light sheet configuration employing lasers and clearing tissue to address a biological question was reported by AH Voie in 1993 in the *Journal of Microscopy*. (AH Voie et al. 1993) They called their method orthogonal-plane fluorescence optical sectioning (OPFOS). This paper studied cleared cochleae, but instead of using well-known software in use at the time for 3-D rendering of confocal microscopy Z-stacks, the authors employed their own custom software yielding wire frame projections, and so the paper did not receive the recognition due. Jan Huisken and Jim Swoger showed the scientific community the true power of LSFM while working in Ernst Stelzer's lab at EMBL Heidelberg (Huisken et al 2004) with Selective Plane Illumination Microscopy (SPIM). Collecting breath taking optically sectioned images of transgenic zebrafish.

Fluorescence is a property of nature that makes objects visible via photons. A photon of a certain wavelength/frequency bombards a molecule and excites one of its electrons to a higher energy state, when the electron relaxes back down to its original state, it releases a photon of a lower energy/longer wavelength. Fluorescence has both advantages and disadvantages. The advantages are:

- When the background is controlled appropriately, fluorescence has the capability to be a very high contrast-enhancement technique
- Fluorescence labeling can be both very sensitive and very specific
- Sensitive fluorescence probes can be applied at low enough concentrations to usefully label structures within living cells and tissues very accurately and in multiple colors.
- Both conjugated antibody labeling and the use of endogenously expressed fluorescent proteins allows cell components to be labeled and their fates traced in living cells.
- Well-proven methods make antibody labeling relatively cheap and straightforward; there are high quality CCD cameras and PMT detectors available to pick up very low fluorescence signals.

These several advantages have made fluorescence microscopy widespread among biologists and biomedical scientists. However, there are three major disadvantages that must be managed and controlled in order to make fluorescence a useful tool.

- The self-luminous nature of fluorophores means that even those above and below the plane of focus (i.e. within the depth of field of the microscope objective) contribute signal to the in-focus image. This results in an unclear image, which gets worse the thicker the sample is.
- Fluorophores will bleach irreversibly after a certain time of continuous or repeated excitation.
- When two or more fluorophores are imaged at the same time, the nature of their excitation and emission spectral profiles means that signal from one fluorophore can ‘bleed-through’ into the detector assigned for a second, longer wavelength, fluorophore.

The first disadvantage is the most serious one, and the confocal microscope was developed (Amos & White, 2003) precisely to manage and to some extent control this problem. For over two decades the confocal microscope has been the workhorse - or at least the default microscope of choice - for optical sectioning. It became available because of three specific requisites: good enough engineering know-how to design the scanning mirrors, cheap enough lasers, and fast enough computing power to integrate this hardware.

At about the same time Linux was made available as an open source operating system, ImageJ also came out around this time. Fiji is a variant of ImageJ that is better suited for the Life Sciences, due to the fact that it is designed with upgrades in mind. The plugins that come packaged with it have been thoroughly tested to ensure robustness.

Why did these two things (newly emergent, widely-used technology and freely-available cross-platform computer code) not come together in some open source confocal system? The reason is due in part to the complexity of rastering the laser beam employed in confocal microscopy. Because Light Sheet Fluorescence Microscopy (LSFM) is a wide field detection technique, it is much simpler to implement. LSFM was developed to address some of the disadvantages apparent in confocal microscopy: it is not possible to image deep into thick tissues with a confocal microscope; photo-bleaching (with accompanying photo-toxicity) is relatively high, and the scanning mirrors coupled to PMT detectors means that image acquisition is relatively slow. The laser slit-scanning and array-

scanning designs were attempts to address the slow speed issues of point-scanning confocal microscopes, whereas the two-photon microscope was developed (Dink *et al.* 1999) to image very thick tissues in depth. LSFM seeks to further overcome the bleaching disadvantage of slit- and array-scanners, and the limitations of acquisition speed and resolving power of the two-photon microscope.

Science is the measure of what mankind knows about itself and the world in which it lives, this knowledge should be freely available to the whole of mankind. This philosophy is collectively known as Open Science (<http://www.openscience.org/blog/>). With this in mind, we make the OpenSPIM platform open to the world. The explanation on our wiki page (<http://www.openspim.org>) states it this way:

*“OpenSPIM is a platform to build, adapt and enhance SPIM technology. It is designed to be as accessible as possible:*

- [detailed, easy-to-follow build instructions](#)
- [off-the-shelf components and 3D-printed parts](#)
- [Modular and extensible design](#)
- [completely open blueprints](#)
- [completely Open Source](#)

*The build instructions are intended to allow scientists without prior knowledge in building optical systems to make their own OpenSPIM set-up. If a 3D printer is not readily available, the parts are designed to be easily machined by any competent workshop. The set-up is small enough to fit inside a [suitcase](#). The software is built on top of the Open Source projects [µManager](#) and [Fiji](#).*

## I.I INTRODUCTION TO LIGHT SHEET FLUORESCENCE MICROSCOPY

LSFM is a very powerful tool for developmental biologists, embryologists, and marine biologists, as it can produce very informative datasets of living systems over the course of hours and days without disturbing or damaging the sample.

### I.I.I PROBLEMS WITH CONVENTIONAL FLUORESCENCE MICROSCOPY

In conventional fluorescence microscopy the microscope objective serves both as the end of the illumination system and beginning of the detection system. This causes problems in a few ways:

- Because the resolution in the final image is tied to the Numerical Aperture (N.A.) of the detection lens, and it is one and the same as the illumination lens, the sample is flooded with copious amounts of light. This is a double-edged sword, as when the N.A. doubles the amount of light that is used quadruples.
- This light excites fluorescently labeled objects above, in, and below the plane of interest. The objects that are above and below this plane are out of focus, which makes the image appear fuzzy when it should be sharp and detailed.
- Since the fluorescent molecules are destructible, the ones outside of the plane of interest become degraded before they are imaged at a better focal plane

Some of these problems are compounded when using a Laser Scanning Confocal Microscope (LSCM). Due to the fact that LSCM utilizes a confocal pinhole in the detection path, the out of focus light from fluorescently labeled objects above and below the focal plane is discarded. This gives superb contrast and detail in the final image, but all of the other problems are still present. In fact, they are sometimes even worse as the amount of excitation light needed is much higher to get the fluorescent signal through the detection pinhole. This destroys the fluorescent molecules and sometimes even the sample.

---

### I.I.2 HOW LSFM IS DIFFERENT FROM CONVENTIONAL FLUORESCENCE MICROSCOPY

By decoupling the illumination and detection axis from the same path, and orientating them perpendicularly to each other, it is possible to illuminate only the focal plane of the detection lens instead of the whole volume being imaged. This is the main idea behind LSFM. Some of the advantages of this are:

- The plane of interest is the only one being illuminated. So out of focus objects in other planes do not disturb the image, as the light did not excite them.
- Very low N.A. lenses are used for the illumination; so much less light is used to excite the fluorescently labeled objects. This leads to longer-lived signal.

Although LSFM can be used on a conventional microscope stand, both upright and inverted, normally the orientation of both the illumination and detection is perpendicular to this axis being parallel to the ground. This is the case in SPIM, which is the design of the system described in this paper.

In SPIM the light sheet is produced by a cylindrical lens that only focuses light in one axis, and continues parallel in the other, creating a line, as compared to a spherical lens that focuses in both axes creating a point. This lens is oriented horizontally due to the fact that after going through spherical lenses it alternates from horizontal to vertical after every element. So at the end of the illumination beam path the light sheet is oriented vertically intersecting the sample parallel to the detector chip.

Lasers are used in the creation of the light sheet for some of their advantageous properties:

- Monochromatic light – for specific excitation of selected fluorescent molecules.
- Tight collimation – parallel beam profiles for non-diverging light sheets.

Another way to create a light sheet is to scan a laser using a galvanometer scanner along one axis very rapidly. This is called Digitally Scanned Light sheet Microscopy (DSLM), which scans a laser beam up and down so fast along the Y-axis that it blurs into a light sheet. This has more deleterious effects in its disadvantages than its advantages:

- The amount of power put into the system is an order of magnitude or two more than with SPIM. Because of this the sample might die in the middle of development or the fluorophores might bleach.
- The temporal resolution has to be tightly matched to the read out of the detector

However, the advantages can be very useful:

- Very interesting beam profiles can be used such as Gaussian, Bessel, and Airy beams. The last two can be focused very thin for submicron axial resolutions.
- The laser can be blanked in certain intervals to create a pattern for Structured Illumination (Wilson *et al.* 1996), which is a method to improve image contrast.

Light sheet microscopy has proven very effective in imaging large specimens with optical sectioning, however there is another approach to whole animal imaging: Optical Projection Tomography (OPT) (Sharp *et al.* 2002). The differences between these two imaging methods is that OPT does not use a light sheet, but illuminates the sample with a transmitted or reflected light much in the same way as conventional microscopy. But the whole specimen is in focus due to the large depth of field of the detection lens. Because of this, the lateral resolution of the lens is much better than its axial resolution. The sample is rotated around a midline that is positioned in the focal plane of the lens so that when the sample turns the midline always stays in the same position. After collecting hundreds of views, a computer algorithm is used to collapse the worse axial resolution to the better lateral resolution. The main problem with OPT is that the samples are usually dead as a doornail.

---

### 1.1.3 SAMPLE MOUNTING

OPT, and most flavors of LSFM, rotate the sample to image other sides (views) of the specimen. In the case of OpenSPIM the sample is suspended in a column of agarose gel surrounded by water instead of squished between a glass slide and coverslip as in conventional microscopy; this is a more “true to life” way of looking at things. It also gives the ability to rotate the sample to observe the other side(s). This is one of the main advantages to LSFM over other forms of optical imaging with the exception of OPT.

This method of sample embedding creates a more isotropic resolution due to the rotation of the sample. The fact that the axial resolution in one view is the lateral resolution in the one of the following views and they can be collapsed down to the lowest common denominator via software plugins. The more views observed, the better the effect. With very high N.A. lenses (1.3 or 1.4 oil) the axial resolution in a Z-stack is around 3-5 times worse than the lateral resolution but can be as high as 10-15 times worse in lower N.A. objective lenses.

Because the column of agarose gel is surrounded by water, the best way to illuminate and detect the fluorescent signal is with water-dipping objectives. Water objectives are limited in the N.A. they can achieve by the Refractive Index (R.I.) of water (1.33). So the very best lens that is available at this time is only around 1.1 N.A..

The R.I of the agarose is nearly identical of that of the surrounding water due to it's being 98-99% water itself. When water-dipping objectives are used, there are fewer problems with light being perturbed in its path by mismatching of R.I. through different materials.

Sub-micron beads are added to the agarose along with the sample before it cures, these beads are used as fiduciary markers while analyzing the data for registering and reconstructing the multiple views based on their nearest neighbors (Preibisch *et al.* 2010). This is similar to recognizing star constellations in the night sky, except that it is in 3D instead of 2D like the star analogy.

When the sample goes through the light sheet, the fluorophores in the beads that surround it are excited. In the stack might be hundreds or thousands of these beads. Since these beads are in other views, surrounding beads can identify them because they have known distances in 3D space based on info from multiple views.

It is also possible to do deconvolution of the data acquired (Preibisch et al. 2014) based on information that these beads give, namely their Point Spread Functions (PSF). Because there are multiple views of these beads, their PSFs can be collapsed even better then with one view.

## 2 MATERIALS AND METHODS

The Materials and Methods section will cover the necessary steps to take to build an OpenSPIM system. The figures in this section are made with Solidworks 3D Computer Aided Design (CAD) software (see **figure 1** as an example), or are window screen shots from the OpenSPIM plugins and software.

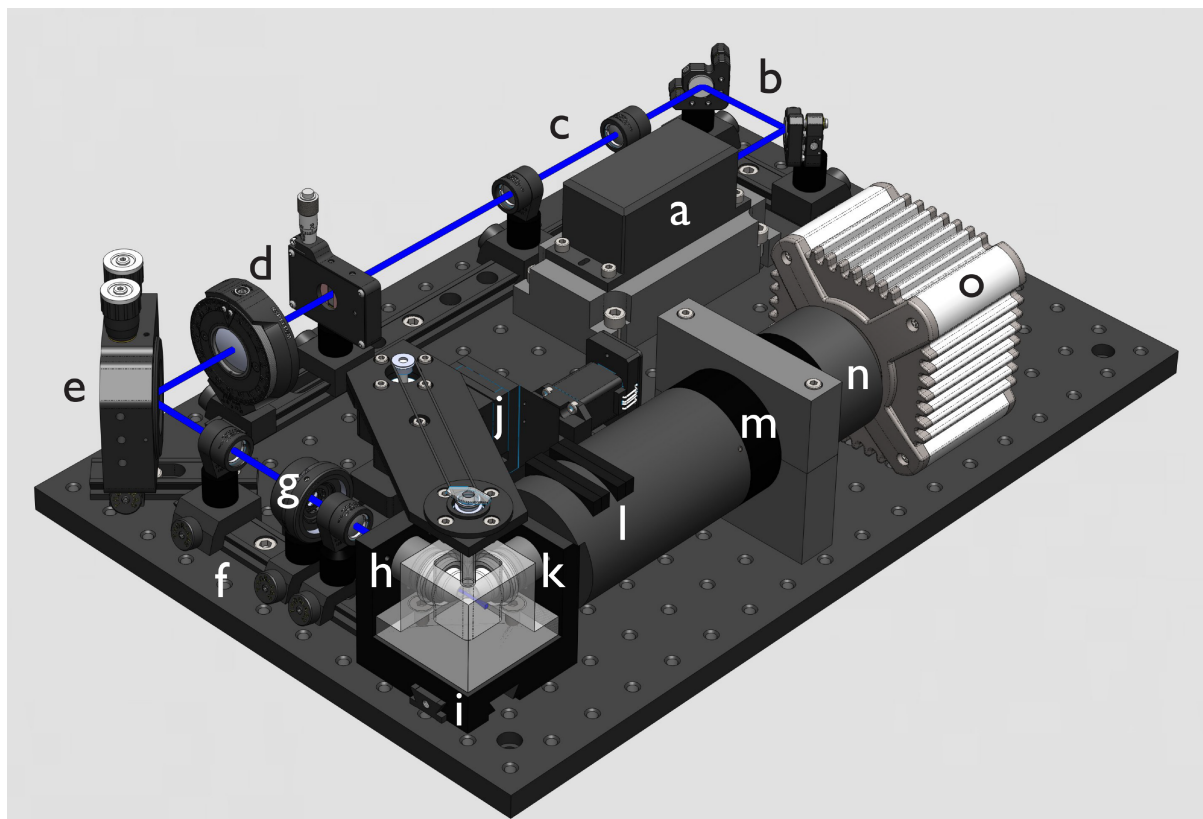


**Figure 1:** Solidworks rendering of the OpenSPIM system with overlaid letters to help with the Materials and Methods section. The laser (a) is on a metal heat sink, it's 1 mm beam gets positioned with two mirrors (b). A 4x beam expander telescope (c) broadens the beam to 4 mm, where it continues through a vertical slit and cylindrical lens (d). This lens focuses a line onto a mirror (e) that is positioned in a conjugate plane to the back focal plane of the illumination objective (h) by means of a telescope (f). An optional iris (g) can be used for shaping the sheet height in the sample chamber (i). A 4D motorized translation stage (j) is used to move the sample through the sheet that is in the focal plane of the detection objective (k). The fluorescence emission filters are placed in the infinity tube (l) also work as a laser block to protect the detector (o), where the image of the sample is formed using the tube lens (m) in the primary image plane where the c-mount (n) hold the detector.

### 2.1 COMPONENTS OF THE MICROSCOPE

OpenSPIM can be easily constructed on an optical breadboard or table, which can be purchased from optical component manufacturers. The principle advantage of open construction on a breadboard is that the tapped holes are equidistant and aligned in rows and column that are machined with tight tolerances so that objects bolted down are either parallel or perpendicular to one another. The system must be configured and built on a specific horizontal plane. All components designed for the OpenSPIM system are raised off the optical breadboard surface by 50 mm. This is

an arbitrary number that can be changed if necessary, as it needs to be looked at carefully when dealing with large cameras.

The light sheet creation method chosen for OpenSPIM is simple; it makes a static light sheet with a cylindrical lens instead of scanning a laser beam with a galvanometer. Light sheet illumination is ideal for a widefield system with an array detector such as a CCD or CMOS camera.

For simplicity the OpenSPIM system can be broken down into 4 subsystems:

- The illumination system
- The sample chamber (which is the intersection of the illumination and detection systems)
- The positioning system
- The detection system

---

### 2.1.1 ILLUMINATION SYSTEM

The illumination system begins at the laser cavity, which can be a gas or solid-state laser. It continues on through a set of optics, which includes two telescope systems, a cylindrical lens, and the illumination objective, which ends as a light sheet in the sample chamber.

---

#### 2.1.1.1 A - THE LASER

The choice of the operation wavelength of the laser that is used depends on the fluorescent molecule that will primarily be used for the imaging of the sample at hand. We chose a 488 nm laser wavelength for our system due to the fact that it works very well for Green Fluorescent Protein (GFP), which is widely used in transgenic *Drosophila* lines.

The small size of solid state lasers such as diode lasers and diode pumped solid state (DPSS) lasers is ideal for this purpose. Gas lasers are much larger and generally have less power.

DPSS lasers overcome some of the disadvantages that diode lasers have such as:

- Diode lasers can fluctuate around the design wavelength due to temperature instabilities ( $\pm 3\text{-}5 \text{ nm}$ )
- They can also produce longer wavelength light (that may fall in the emission spectra as speckle or reflect off of the sample). It seems impossible to measure the amount, but it is still visible for anyone to notice with their own eyes in the case of a 488ish nm diode laser.

It is possible to use multiple lasers with OpenSPIM. A good wavelength pair in cases with genetically modified organisms would be 488 nm and 561 nm, due to the fact that GFP and Red Fluorescent Protein (RFP) are the most widely used. The 405 nm and 640 nm laser lines could be used as well to cover a larger selection of fluorophores in the visible range of the electromagnetic spectrum. Beam combining is necessary when using more than one laser line; this can be achieved using dichromatic mirrors in “step” configuration to bring all the lines into the same beam. This feature is not yet implemented in OpenSPIM.

#### 2.1.1.2 B – TWO MIRROR LASER POSITIONING SYSTEM

Two kinematic mirror mounts are used to position the laser in the correct optical axis of the beam expanding telescope, the vertical slit, the cylindrical lens, and the gimbal mirror mount.

#### 2.1.1.3 C - BEAM EXPANDER (FIRST TELESCOPE SYSTEM)

A beam-expanding telescope is used for free space optics. The trick is to fill the cylindrical lens' back aperture with a big enough diameter so that the light sheet will be thin and tall enough. 4 mm diameter seems to be best for the system, both theoretically and practically. This will be further discussed in the results section 3.1.

In a free space laser system, the beam-expanding telescope uses a shorter focal length first lens ( $L_1$ ) and a longer focal length second lens ( $L_2$ ) to magnify the input beam to a larger diameter. This is unlike a telescope for magnifying an image of a distant object, which has a longer focal length first lens and a shorter second lens. To get the effective magnification of a telescope system the focal length of the first lens is divided into that of the second.

For example, with a 1 mm beam diameter, a **50** mm focal length first lens and a **200** mm second lens would make a **0.25x** magnification. This would result in an image of an object to appear smaller than itself, but also expanding a parallel beam to 4x its diameter. Due to the small diameter of the lenses that we chose for the original OpenSPIM (1/2" – 12.7 mm), we use a **19** mm first lens and a **75** mm second lens making the effective magnification **3.95x**. There is a rule of thumb in optical technology development that I were unaware of at the time of designing the system, which states that focal lengths less than 25 mm should not be used due to lens aberrations. But I have yet to see a real problem with this though.

#### 2.1.1.4 D - CYLINDRICAL LENS AND VERTICAL SLIT ASSEMBLY

The cylindrical lens ( $f=50$  mm) is oriented in a horizontal fashion, its effective aperture is limited to the axis it is oriented in. This aperture is filled with  $\pm 4$  mm of light. The vertical slit sits between the expanded beam and cylindrical lens acts as an aperture limiter. It affects how wide of a beam of light falls on the horizontal axis of the cylindrical lens. This affects the thickness of the light sheet in the sample chamber, the wider the opening the thinner the light sheet but with deleterious affects to the waist at the edges of the field of view (FOV) of the detection system. The thinner the slit opening the more homogeneous the light sheet is across the whole FOV but at the cost of a thicker light sheet.

#### 2.1.1.5 E - ADJUSTABLE AXIS GIMBAL MOUNT MIRROR

The surface of the mirror is where the cylindrical lens is focused sharply (although its distance to the mirror does not seem to play a major role in light sheet quality), and it is rotated  $45^\circ$  in the direction of the sample chamber. Due to the fact that the next telescope system is focused on the back focal plane of the illumination objective, and to the surface of the mirror, they both are conjugate planes to one another. Because of this, when you move the mirror you also move the light sheet inside the sample chamber. This makes life a lot easier when aligning the system. See section 3.1

### 2.1.1.6 F - CONJUGATE PLANE TELESCOPE SYSTEM (SECOND TELESCOPE SYSTEM)

The difference between the beam expanding telescope system and the conjugate plane telescope system is that the light entering and exiting the system is either parallel, as with the beam expanding telescope, or focused on a focal point/plane, as with the conjugate plane telescope. This is its primary function, to focus the Back Focal Plane (BFP) of the objective into a conjugate plane with the mirror in the Gimbal mount.

### 2.1.1.6.1 G - IRIS APERTURE STOP (OPTIONAL)

This is an optional piece that sits in the middle of the conjugate plane telescope system, where the two focal points of the lenses converge. It has the affect of shortening the height of the light sheet in the sample chamber. This can be useful if one wants only to illuminate what the detector can observe.

### 2.1.1.7 H - ILLUMINATION OBJECTIVE

The ideal illumination objective would have a reasonably long working distance (WD) (3-5 mm), a low magnification, outside dimensions that facilitate an “up close and personal” pairing (perpendicular yet sharing the same volume of other focal points of neighboring objectives), and relatively low N.A. We use the Olympus UMPLFLN semi-apochromat 10x/0.3 objective lens because it has these characteristics; it has a 3.5 mm WD. The back aperture is never even close to being completely filled with the illumination system, so generally it uses less than 0.1 N.A. in the axis of the cylindrical lens focus and much less in the other axis. This makes the depth of field very long, which in turn leads to a more homogeneous light sheet thickness.

## 2.1.2 I - SAMPLE CHAMBER ASSEMBLY

The sample chamber (see **figure 2**) is where all of the action happens. It is a watertight container that has at least two (but could have as many as 3 or 4) water dipping microscope objectives oriented perpendicularly (and collinearly in the case of 3 or 4 lenses) to each other conjoining their respective focal points/planes. For sake of clarity we refer to a 2 lens system as an “L” configuration, a 3 lens system as a “T” configuration, and a 4 lens system as a “X” configuration based on the convergence of their axes and how they resemble the letter assigned to it.

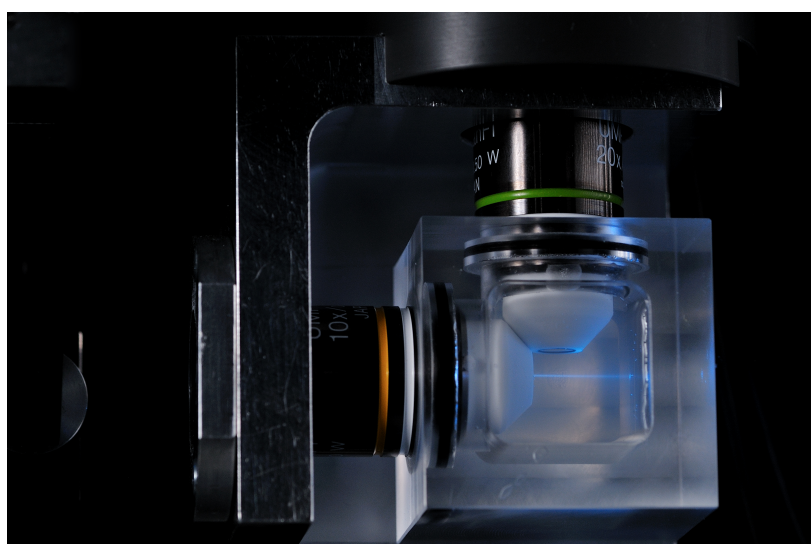


**Figure 2:** Sample chamber assembly with light sheet. The original L-OpenSPIM design uses only 2 objectives.

### 2.1.2.1 CHAMBER BASE

The base of the chamber is made out of a solid piece of material, such as metal or robust plastic. The width and length of the chamber are related to the length of the objective being used. It is always longer than one length, but never longer than two. Because a RMS standard objective lens is 45 mm from the flange to the working distance, the chamber of a single sided illumination and detection system would be around 60-70 mm depending on the design of the chamber. This is due to the barrel diameter of the objectives used being ~20 mm. On a double-sided system it would be 90 mm due to the fact that the focal planes of the juxtaposed objective lenses would meet in the middle. With larger and longer bodied objectives such as many of the new low to middle magnification (16-25x) water dipping lenses with high N.A. (0.75-1.1) the same rule would have to apply. For instance, the Nikon CFI75 LWD 16x/0.8 has a 75 mm length so

### 2.1.2.2 SAMPLE CHAMBER

The sample holder is designed to keep the water dipping lenses submerged in water with out it leaking out. Depending on how many lenses will be used will determine the amount of holes drilled around it's 4 sides, and whether O-rings are necessary or not. O-rings are gaskets like rings with a circular band of rubber, they need to have a wider diameter ring in the middle of the chamber walls to compress the O-ring around the objective with enough force to make any water leakage impossible. We make the chamber out of a clear acrylic plastic for its transparent properties. It is enough so that one can see where the sample is by looking through the chamber wall, but this only makes sense when using an L or T variant of the OpenSPIM system. With an X variant it would be advisable to use a matte black robust material, that way there is less chance of stray light from entering any of the objectives surrounding the sample.

### 2.1.2.3 WATER-DIPPING MICROSCOPY OBJECTIVES

Any water dipping microscopy objectives can be used, as long as the focal planes of both the illumination and detection objectives meet in the plane of interest, and they don't overlap or touch each other. The best design lenses that we have found are for electrophysiology, due to the fact that they have bodies less than 45° from the optical axis. This way it is possible for them to be oriented perpendicular to one another.



So far we have used Olympus UMPLFLN water dipping lens line to great effect (see **figure 3**). This line of objectives that are similar in dimensions (10x/0.3, 20x/0.5, and 40x/0.8) covers most developmental biologist and embryologists dream list of magnifications. I have also designed a chamber with the Nikon CFI75 LWD Plan Fluorite 16x/0.8 lens for detection that also happens to meet this criterion.

**Figure 3:** Water-dipping microscopy objectives

### 2.1.3 J - SAMPLE POSITIONING SYSTEM

The 4D Motor System that we use for OpenSPIM is made by Picard Industries in Albion New York (see **figure 4**). I originally chose them based on the fact that individual motors were about an eighth

the price of what everyone else was using at the time. After fiddling around with a configuration that worked for positioning, I found my design to be flimsy. I then asked Picard Industries to use my design to build a system that is more robust. Their system is now the one that we use on our

OpenSPIM, because it is much more stable and robust. It has 3 translation motors that move in X, Y, and Z in  $1.5 \mu\text{m}$  steps over a 9 mm range, and a rotation motor that rotates the sample around the Y-axis in  $1.8^\circ$  steps (or 200 positions per rotation). The X-axis is, from the point of view of the camera, left and right. The Y-axis is up and down, while the Z-axis is back and forth.

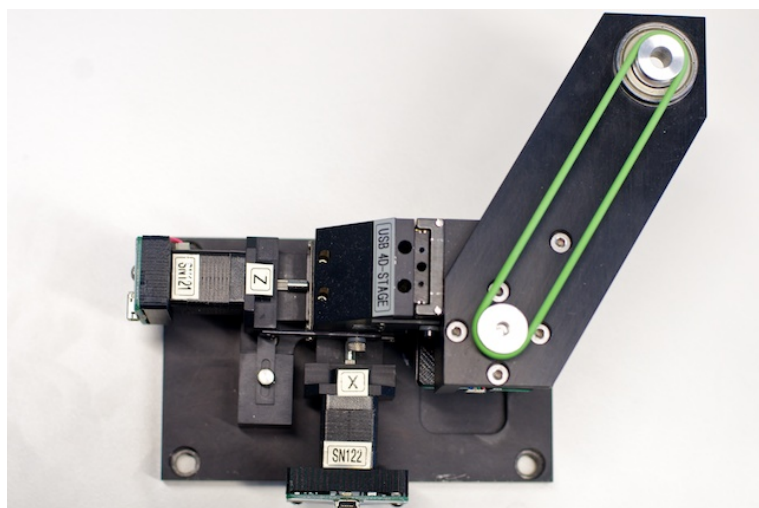


**Figure 4:** Sample Positioning system

#### 2.1.4 DETECTION SYSTEM

The detection system consists of a detection lens, and infinity space tube for optical elements such as filters, an optional magnification wheel, a tube lens for the detection objective, a c-mount (with a 0.5x or 1.0x magnification), and a wide field detector.

##### 2.1.4.1 K - DETECTION OBJECTIVE

As stated above, there are two chamber designs for different detection objectives: one for the standard Olympus UMPLFLN objective line, and one for the Nikon CFI75 LWD Plan Fluorite 16x/0.8 lens.

The UMPLFLN 10x/0.3 and the 20x/0.5 have the same working distance (3.5 mm), whereas the LUMPLFLN 40x/0.8 has a 3.3 mm working distance. This does not matter due to the fact that all of these lens bodies have a  $45^\circ$  bodies from the optical axis, so the LUMPLFLN 40x/0.8 just sits a little closer to the sample.

The 10x/0.3 has a larger field of view optimal for larger samples such as Zebrafish embryos ( $\pm 1 \text{ mm}$ ), but the N.A. is not very good. Another way to enlarge the field of view is to use a 0.5x de-magnifier c-mount on the 20x/0.5, this gives better resolution at the cost of collecting less light. It also does not work well for larger chip detectors such as the Andor/Fairchild/PCO sCMOS that recently came to market.

The 20x/0.5 is our choice lens for observation of Drosophila ( $\pm 500 \times 200 \mu\text{m}$ ) embryogenesis. This happens to be an all around good lens for most samples, as the N.A. is acceptable for the majority of the work. As stated above, it is possible to use extra magnification. We have used de-magnification in the form of a c-mount and magnification in the form of a multiple magnification wheel (see **figure 6**) with 4 positions: 1.0x (empty), 1.25x, 1.6x, and 2.0x.

The last Olympus lens has the highest magnification for the smallest objects, and also the best resolution. The 40x/0.8 could be used for sea urchin embryos or anything else that is relatively small ( $\pm 300$  um).

The Nikon CFI75 LWD Plan Fluorite 16x/0.8 lens has a very large field of view with the same resolving power of the 40x/0.8, but costs twice as much. But given the specifications, it is a bargain. With this lens, if everything is ideal, one could image a large sample with the resolution of a small sample.

Both Japanese microscopy optics companies Olympus and Nikon design their objectives to be corrected so that any normal tube lens of the right focal length will form a corrected image. The same cannot be said for Carl Zeiss Microscopy and Leica Microsystems; both of these German companies correct the final image after the tube lens. This is one of the reasons I decided against using their objective lenses.

#### 2.1.4.2 L - INFINITY SPACE TUBE AND OPTICAL FILTERS

The infinity space tube is a simple tube cut to the length of the recommended distance between the objective lens and tube lens. We have cut into the infinity space tube (see **figure 5**) multiple slots for using microscopy grade filters for blocking laser excitation light from ever reaching the detector and for collecting as much fluorescent light as possible to form the image on the detector. Depending on what laser(s) one chooses is the determining factor on which filter(s) to buy. For example, if there is only one laser line a single band pass filter or long pass filter that opens up 5-10 nm away from the laser line would suffice. But if there are multiple laser lines then a multi band pass filter would be best.



**Figure 5:** Infinity space tube and optical filters

#### 2.1.4.2.1 MULTIPLE MAGNIFICATION CHANGER WHEEL (OPTIONAL)



This is an optional piece that can give you the ability to zoom in a bit closer to the sample, but at the cost of signal intensity. It has four positions that magnify the image by 1.0x, 1.25x, 1.6x, and 2.0x, (see **figure 6**) which can come in very handy in certain situations. For example, with the 20x/0.5 it would be possible to image at the native magnification as well as at 25x, 32x, and 40x without ever changing the objective.

**Figure 6:** Multiple magnification changer wheel (optional)

#### 2.1.4.3 M - TUBE LENS

The tube lens is used to focus the infinity corrected parallel light beam that comes out of the back of the objective to an image at the imaging plane where the detector sits. The focal length of this lens depends on the objective that it is used with. Olympus objectives use a 180 mm focal length, while Nikon objectives use a 200 mm focal length. Zeiss and Leica require proprietary tube lenses.

#### 2.1.4.4 N - C-MOUNT

A C-mount adaptor is used to place the detector in the imaging plane in a robust manner. Olympus produces a few different magnifications, but only two are really interesting for an OpenSPIM with their lenses: the 0.5x de-magnifier can give more field of view than the 1.0x, but at the cost of loss of light due to the glass elements inside of the unit.

#### 2.1.4.5 O - DETECTOR

The detector is the last element in the detection path. It can be a scientific grade CCD or CMOS chip, or any other type of wide field detection imaging device.

#### 2.1.4.5.1 NYQUIST SAMPLING

The optimum (Nyquist) sampling frequency depends upon the microscope, the objective and the size of the sensor in the detector.

I find that it sometimes causes problems in understanding when discussing “pixel” size. Pixel means picture element, which means that it only applies to the image. A detector element, or dixel, is a better descriptor for cameras than pixel could ever be.

Ideally, the dixel size should be equal to, or less than half the size of the smallest resolvable distance of the objective used (Rayleigh's equation:  $d=0.61 \times \text{wavelength}/\text{N.A.}$  or  $\text{distance} = 0.61 \times \text{wavelength}/\text{N.A.}$ ). Nyquist's *minimum* requirement becomes 2.3 dixels per minimum resolved unit, but a slight over sampling can be advantageous (2.5-3.0 is acceptable).

In table I the differences between the water-dipping objectives that have already been described in this dissertation are charted along with different magnification possibilities. The dixel size used in table I is 6.45  $\mu\text{m}$ . This is the same size as the ICX-285, Sony's interline CCD chip that has long been the gold standard for fluorescence microscopy. The number seen in the box is the pixel size (in  $\mu\text{m}$ ) in the image. The wavelength of the light that is assumed to be is 550 nm, as it falls in the middle of the visible spectrum in the green range and is a good representation of generalizing the resolution of an optical element.

A table of pixel sizes of different magnifications.	Theoretical Resolution	0.5x	1.0x	1.25x	1.6x	2.0x
UMPLFLN 10x/0.3	0.486	1.290 (5x)	0.645 (10x)	0.516 (12.5x)	0.403 (16x)	0.323 (20x)
UMPLFLN 20x/0.5	0.292	0.645 (10x)	0.323 (20x)	0.258 (25x)	0.202 (32x)	0.161 (40x)
LUMPLFLN 40x/0.8	0.182	0.323 (20x)	0.161 (40x)	0.129 (50x)	0.101 (64x)	0.081 (80x)
LWD 16x/0.8	0.182	* 0.806 (8x)	0.403 (16x)	* 0.323 (20x)	* 0.252 (25.6x)	* 0.202 (32x)

**Table I:** A table of pixel sizes of different magnifications. The Y-axis corresponds to the different water dipping detection lenses we have used, and the X-axis of extra.magnification filter wheels and or de-magnifying c-mounts. The wavelength of the light assumed is 550 nm (0.55  $\mu\text{m}$ ), and the assumed dixel size is 6.45  $\mu\text{m}$ .

## 2.1.5 SELF MADE COMPONENTS

### 2.1.5.1 I - SAMPLE CHAMBER, CHAMBER BASE, AND THREADED OBJECTIVE RINGS

The sample chamber is cut out of a piece of clear acrylic plastic with holes on perpendicular faces that have a slightly bigger diameter than the water dipping objectives. Inside the walls of the holes are grooves cut around the circumference to hold a rubber O-ring that makes a watertight seal around the objective.

The chamber base is what holds both the objectives, along with the threaded objective rings, and the sample chamber in place.

### 2.1.5.2 L - INFINITY SPACE TUBE AND FILTER HOLDERS

The infinity space tube that we designed is the same diameter as the Olympus tube lens and C-mount at 60 mm. There are two slots that have a inside dimension of 40 mm wide by 10 mm thick that take a filter holder that has very similar outside dimensions. The filter holder consists of two pieces that are mirrored to each other that can take a 25.4 mm diameter by 3.5 mm thick optical filter.

### 2.1.5.3 INFINITY SPACE TUBE HOLDER

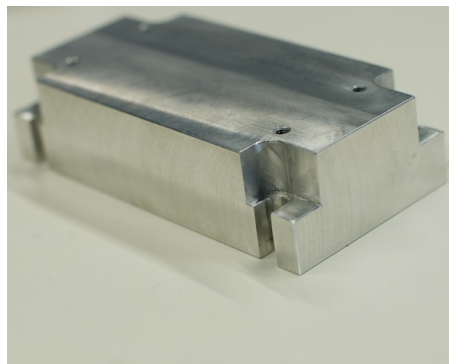
The infinity space tube holder is a assembly of two parts: a base piece that raises the tube 50 mm off the optical bread board, and a top piece that clamps the tube down tightly. This can be made out of almost any hard material like PVC or metal.

### 2.1.5.4 STILTS

These stilts are made to bring the optical elements off of the surface of the optical breadboard by 50 mm, but most of these components are on a rail system anyway so they can only travel along one axis. They vary in length depending on the component that is being lifted. The material used to make these stilts is of little importance, as long as the heights are correct. In fact, they can be 3D printed.

The 1/2" mirror stilts are 16.22 mm tall, the 1/2" spherical lens mount stilts are 14.95 mm tall, the vertical slit stilt is 13.17 mm tall, and the optional 1" Iris mount is 11.16 mm tall.

### 2.1.5.5 LASER HEAT SINK



The laser heat sink has two purposes: it elevates a free space laser output to 50 mm off the surface of the breadboard, and it acts as a thermal heat sink that saps the heat away from the laser so its output is stabilized. It must be made from a solid piece of metal such as aluminum (see **figure 7**).

Fiber coupled lasers do not have to have a heat sink with a 50 mm height, but their ~4 mm collimators do. The collimator takes the place of a free space laser's beam expander.

**Figure 7:** Laser heat sink

## 2.1.6 PURCHASED ITEMS: BREADBOARD, RAIL SYSTEM, OPTICAL MOUNTS...

We purchase most, if not all, of our components from ThorLabs. It was an arbitrary decision based on advice and experience from other optical system developers. We do not have any commercial or financial interests in the company, nor will we seek it. Their snack boxes with trail mix and gummy bears are an added benefit though.

### 2.1.6.1 M6 TAPPED OPTICAL BREADBOARD

The original L-OpenSPIM that we designed fit on a 300 x 450 mm (1' x 1'6") M6 tapped optical breadboard, this is the design that is on the OpenSPIM wiki. Having an actively damped optical table would always be the best option, but if the money is not accessible for one then a simple breadboard works very well.

### 2.1.6.2 RAIL SYSTEM

A rail system can be a mixed blessing/curse. It makes life easier when aligning optical axes, but freedom to put the optics wherever one wants is severely limited. The rail carriers and optical mounts of this system are mated together with self-made stilts to raise the optical elements 50 mm off the breadboard.

### 2.1.6.3 OPTICAL MOUNTS: 1/2" & 1" LENS AND MIRROR MOUNTS

Due to the small size of the original design, the system made use of small optical components such as the 1/2" line from ThorLabs. In certain places we use 1" optic mounts, such as the conjugate plane mirror and the optional iris aperture stop.

## 2.2 DESCRIPTION OF ASSEMBLY STEPS

A much more thorough step-by-step description of the OpenSPIM system assembly can be found on our wiki at <http://www.openspim.org> under the table of parts section, but for sake of completeness the following section will give an overview of the steps.

### 2.2.1 ASSEMBLING THE COMPONENT ASSEMBLIES

There are a lot of small parts, both self made and purchased, that are assembled into larger assemblies that need to be made first before the construction of the system on the optical breadboard happens.

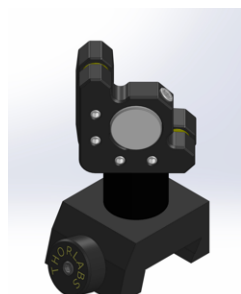
#### 2.2.1.1 RAIL CARRIER STILT AND OPTICAL COMPONENT ASSEMBLIES

There is a variety of rail carrier optical component assemblies that need to be made on the next page and a half.

##### 2.2.1.1.1 1/2" KINEMATIC MIRROR MOUNT & 16.22 MM STILT TO RAIL CARRIER

Two assemblies are needed to adjust the laser beam correctly along the desired optical axis.

Kinematic mirror mounts have either two or three threaded screw shafts, but always three contact points, and behave like a door on a hinge. If the mount has only two threaded screw shafts then they will be positioned opposite each other across the mirror. The third point is located in a position that is at the place where the two other points, if lines, would meet at a right angle. Sometimes the third point also has a threaded screw shaft, this gives the ability to translate the whole mirror forward by a few mm.



When one rotates a threaded screw shaft it translates the mirror either forward or backward depending on the direction of rotation, the other two points are where the mirror mount will pivot. **Figure 8** is a CAD rendition of the assembly.

**Figure 8:** Kinematic mount assembly

#### 2.2.1.1.2 1/2" SPHERICAL LENS & 14.95 MM STILT TO RAIL CARRIER

---



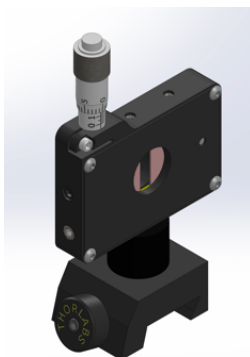
Four assemblies are needed for two telescope systems: the beam expander telescope, and the conjugate plane telescope.

The beam expander telescope uses a 19 mm focal length lens for the first lens, and a 75 mm focal length lens for the second. The conjugate plane telescope uses a 25 mm focal length lens for the first lens, and a 50 mm focal length lens for the second. **Figure 9** is a CAD rendition of the assembly.

**Figure 9:** Spherical lens assembly

#### ADJUSTABLE VERTICAL SLIT & 13.17 MM STILT TO RAIL CARRIER

---



One assembly is needed for the vertical slit to adjust the amount of light that falls onto the back aperture of the cylindrical lens. Because closing the slit shut out the rays capable of higher NA areas of the lens. **Figure 10** is a CAD rendition of the assembly.

**Figure 10:** Slit assembly

#### 2.2.1.1.3 ROTATABLE CYLINDRICAL LENS MOUNT TO MODIFIED RAIL CARRIER

---



One assembly is needed to hold the 50 mm focal length cylindrical lens in place. It needs to be rotated to a horizontal position. There are two small screws on the front of the indexed face of the mirror mount, loosen them and align the rotating face to line up at either 0° or 90° with the reflection you see off the cylindrical lens making sure to lock the screws back to tighten the face down again. **Figure 11** is a CAD rendition of the assembly.

**Figure 11:** Cylindrical lens assembly

#### 2.2.1.1.4 1" GIMBAL MIRROR MOUNT 1.5 MM THICK WASHER TO RAIL CARRIER

---

One assembly is needed to reflect the focused cylindrical light to the conjugate plain telescope.



A gimbal mount is a two-axis mount that pivots at the center of the mirror. The main difference between it and a kinematic mount is that the whole mount assembly must be moved forward or back, as the center point is not translated forward. **Figure 12** is a CAD rendition of the assembly.

**Figure 12:** Gimbal mount assembly.

#### 2.2.1.1.4.1 ADJUSTABLE IRIS & 11.16 STILT TO MODIFIED RAIL CARRIER

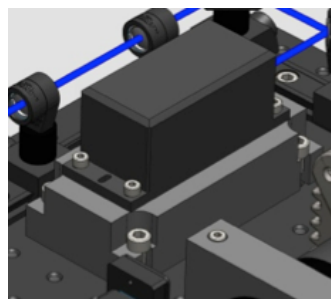
This optional assembly is for adjusting the height of the light sheet so that only the field of view is illuminated during imaging.



Adjusting this component's aperture will determine the height of the light sheet in relation to the field of view of the camera; if one opens it up all the way it will make a taller light sheet height, whereas if you close it all the way down it will make the light sheet height very short. The ideal position is when the height of the light sheet is matched with the height of the camera. **Figure 13** is a CAD rendition of the assembly.

**Figure 13:** Iris assembly.

#### 2.2.2 A - LASER TO HEAT SINK



After getting the heat sink made for the laser the mating of the two pieces should be done carefully. Using heat transfer paste, smear on the top surface of the heat sink and the bottom surface of the laser with latex gloves. Then place the laser on the heat sink being careful to align the holes for screwing the laser down to the heat sink. After screwing the laser down, remove any excess heat transfer paste being careful not to get any on your hands. **Figure 14** is the position of the assembly on the rail system.

**Figure 14:** Laser on heat sink in its position on the board

#### 2.2.2.1 LASER HEAT SINK ASSEMBLY TO BREADBOARD

Place the laser heat sink assembly on the breadboard and use 4 M6 capscrews to tighten it down to the breadboard.

#### 2.2.3 RAILS TO BREADBOARD

Place the correct rails along the row or column that they belong on, and then use at least two M6 capscrews for each rail to tighten them down to the breadboard. This can be found on the wiki at: [http://openspim.org/Install\\_illumination\\_axis\\_on\\_the\\_optical\\_breadboard\\_Part\\_I#Mount\\_dovetail\\_rails\\_onto\\_optical\\_breadboard](http://openspim.org/Install_illumination_axis_on_the_optical_breadboard_Part_I#Mount_dovetail_rails_onto_optical_breadboard)

#### 2.2.4 B - 1/2" KINEMATIC MIRROR MOUNT ASSEMBLIES TO RAIL

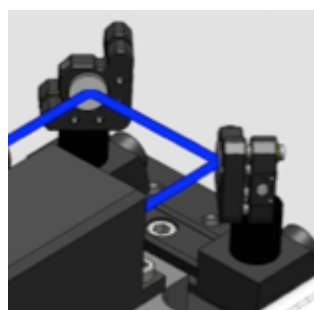


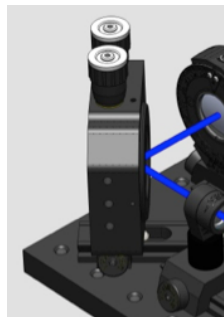
**Figure 15:** position of beam steering mirrors on the rail system

Install the first 1/2" kinematic mirror mount assembly in front of the laser output and roughly rotate the mirror mount 45° toward where you will face the other 1/2" kinematic mirror mount assembly. Install the second 1/2" kinematic mirror mount assembly in a place where it will reflect the light parallel to the laser output by rotating the mount -45°. The distance between the mirrors is not critical, but the second mirror

should be positioned in a place along the rail that reflects the beam down a row or column along the breadboard due to the rails being along the same axis as the optical train of components. **Figure 15** is the position of the assembly on the rail system.

---

#### 2.2.5 1" GIMBAL MIRROR MOUNT ASSEMBLY TO RAIL.



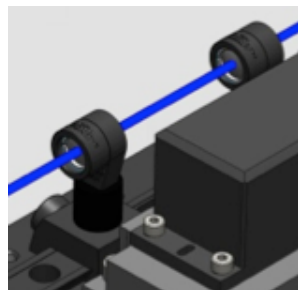
The gimbal mount assembly should be installed in an easy to access place, as this is the most important tool piece in the whole setup. It is positioned along the same row or column that the second 1/2" mirror assembly was aimed down, then it is rotated 45° toward the sample chamber's illumination lens. With these three mirror assemblies in place, the rough laser alignment can be made. This is described in the next subsection. **Figure 16** is the position of the assembly on the rail system.

**Figure 16:** position of conjugate plane mirror on the rail system

---

#### 2.2.6 1/2" LENS ASSEMBLIES TO RAIL – BEAM EXPANDING TELESCOPE

If using a free space laser beam, install the first lens assembly of the beam expander telescope, with the short focal length, shortly after the second 1/2" mirror. Then install the second lens assembly of



the beam expander telescope the sum of the focal lengths away from the first in the direction of the 1" gimbal mirror mount. With the laser turned on and rough aligned (see next subsection), vary the distance between the two lenses until the output is the same diameter along the whole axis. Parallel in parallel out. **Figure 17** is the position of the assembly on the rail system

**Figure 17:** position of beam expanding telescope on the rail system.

---

#### 2.2.7 1" CYLINDRICAL LENS ASSEMBLY TO RAIL

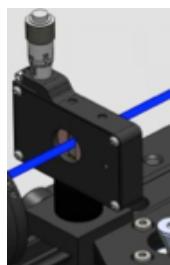


Install the 1" cylindrical lens one focal distance away from the 1" gimbal mirror mount, between it and the beam-expanding telescope. Vary the distance between the two ever so slightly, making sure that the laser focuses to a sharp line on the mirror. **Figure 18** is the position of the assembly on the rail system

**Figure 18:** position of cylindrical lens assembly on the rail system

---

#### 2.2.8 VERTICAL SLIT ASSEMBLY TO RAIL



Install the vertical slit assembly one focal length behind the 1" Cylindrical lens assembly, between the cylindrical lens and the beam expander telescope. It does not really matter where the slit is as the light is parallel, but it is a good practice to keep optics par focal when possible. **Figure 19** is the position of the assembly on the rail system

**Figure 19:** position of adjustable vertical slit assembly on the rail system

---

## 2.2.9 1/2" LENS ASSEMBLIES TO RAIL – CONJUGATE PLANE TELESCOPE



The conjugate plane telescope is a 4f system, in other words every focal plane in the system lies over top of the last one. Install the first lens assembly one focal distance away from the 1" gimbal mirror mount. Then install the second lens assembly the sum of both lens assemblies focal lengths away from the first, now it should be very close to the back focal plane of the illumination objective. **Figure 20** is the position of the assembly on the rail system

**Figure 20:** position of Vertical slit assembly on the rail system

---

## 2.2.10 ADJUSTABLE IRIS ASSEMBLY TO RAIL (OPTIONAL)

Install the adjustable iris assembly the space between the conjugate plane telescope's two 1/2" lens assemblies focal lengths, making sure that it is in the focal planes of both lenses.

### 2.3 LIGHT SHEET ALIGNMENT

Aligning the light sheet is the most time consuming part of the building process, but it does get easier with time and experience. There are two levels of alignment: during the construction phase a rough alignment is necessary, and right before imaging a detailed fine-tuning is highly recommended.

The rough alignment is performed during the construction before any refractive optical elements are installed, but after the mirrors are. Two alignment disks are used in the same assemblies as the 1/2" lenses. One on each end of the optical axis as far apart as they can possibly be from one another, and as close to the mirrors as they can get. This way the angle is as tight as it can be along this axis. Adjusting the mirrors will position the beam correctly so that it is traveling along the optical axis. Do this for both arms of the illumination light path: from the second 1/2" kinematic mirror mount to the 1" Gimbal mirror mount, then from the gimbal to the illumination objective. When this first step is done the optical elements such as the beam expander telescope, cylindrical lens, and conjugate plane telescope can be placed into the beam path in their respective places. For video tutorials see [http://www.openspim.org/Alignment\\_of\\_laser](http://www.openspim.org/Alignment_of_laser)

After the beam expander telescope is installed and checked for a parallel output, the conjugate plane telescope is ready to be put on. Taking care not to forget the fluorescence filter, and not installing the cylindrical lens, turn the laser and camera on. Put a bead agarose solution sample in the chamber, and focus on the capillary's edge. Push out the bead agarose gel out of the capillary into the water filled chamber. Then find the focused light inside the bead solution and bring it to sharp focus with the horizontal gimbal mirror mount knob (Z axis in relation to the detection lens). Adjusting the distance between the conjugate plane telescope lenses will change the focal plane where the light is focused in front of your camera (X Axis of detection lens), while adjusting the vertical gimbal mirror mount knob will position the beam in Y. Once the light cones are centered and focused in the middle of the field of view of the camera chip, the cylindrical lens can be installed.

The fine-tuning of the light sheet happens after everything is built and roughly aligned. This alignment is all done after the Conjugate plane mirror on the second illumination axis. See: [http://www.openspim.org/Advanced\\_Laser\\_Alignment](http://www.openspim.org/Advanced_Laser_Alignment)

A mirror grating, we use a calibrated microscopy grid, is hung between the objectives of the sample chamber brought into focus with the detection objective and rotated 45° into the direction of the illumination arm that will be adjusted (this will reflect the light sheet into the detector). The grid will now have a very thin plane near the center that is in focus. If this signal is too intense consider using a neutral density filter to attenuate the light.

Once this is done the laser is turned on, and the intensity tuned down to around 1 mW or even less. Depending on the laser properties, the cleanup filter should be removed from the illumination path while taking care that the emission filter is still in the detection path to protect the detector unit from too much light. If the rough alignment was done correctly, there should be a vertical patch of light on or around the plane of focus.

Using the conjugate plane mirror in the gimbal mount, adjust the horizontal knob so that the vertical patch is translated to where the focal plane is. Then finally adjust the conjugate telescope's lenses to make the vertical patch as narrow as possible. Once this is done, make a z-stack of the grid mirror so that the focal plane goes from one side of the field of view to the other. The thickness of the light sheet on the edges are much larger than in the middle if the vertical slit behind the cylindrical lens is opened too far, to fix this adjust the width of the slit opening to a place where the vertical patch is more or less homogeneous across the range of the z-stack.

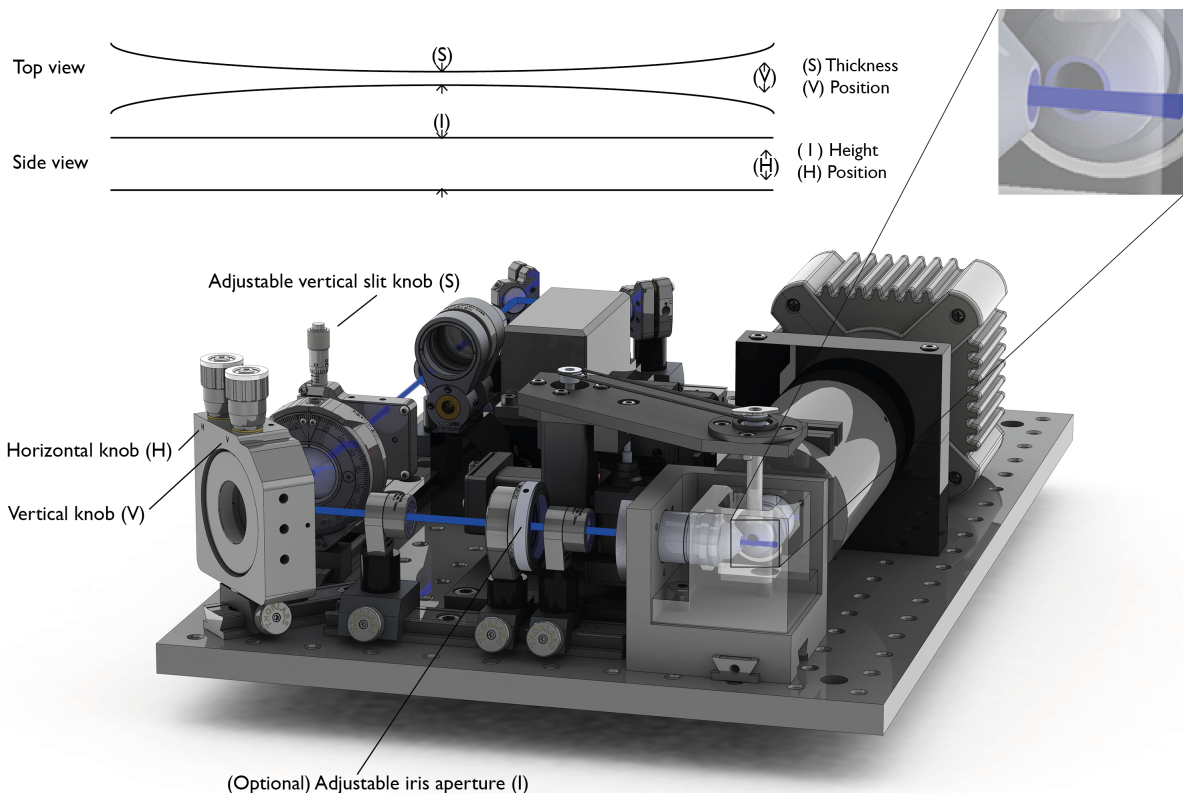


**Figure 21:** Light sheet alignment in regards to the use of the adjustable rotation knobs, and their function.

## 2.4 SAMPLE PREPARATION

Since the sample is suspended in a matrix gel column such as agarose, the sample preparation is noticeably different from conventional microscopy. Capillaries and plunger rods are used instead of glass slides and coverslips.

Samples such as insect embryos must first be dechorionated before imaging due to intense light scatter of the outer chorion. With *Drosophila melanogaster* a 50/50 chlorine bleach water solution mix is made for the job. Submerging the embryo for two minutes will dissolve the chorion. A liberal amount of rinsing is necessary for making sure no more bleach water mix solution stay behind.

A low melting point agarose is made then brought down in temperature (to  $\pm 35^\circ \text{C}$ ) until it almost solidifies (at  $25^\circ \text{C}$ ) and is kept at there until the sample is submerged. Sometimes sub resolution beads are added to the solution for multi-view imaging. Then a plunger rod is inserted all the way through a 20 – 200  $\mu\text{l}$  glass capillary tube till it pokes out of the other end. That end of the capillary is inserted into the agarose solution where the sample is. Using capillary forces, the plunger rod is pulled up, pulling the sample along with agarose into the capillary. The whole apparatus is then left to cure for 5-10 minutes. It is then ready to image.

We implemented an interesting way to hold the sample capillary that utilizes a simple 1 ml syringe container (see **figure 22**) and two of the same plunger pistons that comes with it. Also see our wiki: [http://openspim.org/Drosophila\\_embryo\\_sample\\_preparation](http://openspim.org/Drosophila_embryo_sample_preparation)

**Figure 22:** Sample holder

## 2.5 OPERATION OF THE MICROSCOPE

We use two open source software packages for our acquisition and image post processing:

The first is called Fiji (Schindelin et al. 2012); it is an offshoot of ImageJ, which is widely known and used in biological sciences due to its ability to use self-made plugins for different tasks. **Figure 23** shows the main window of the program.

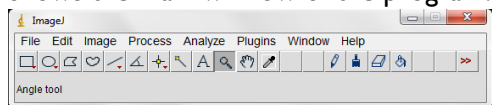
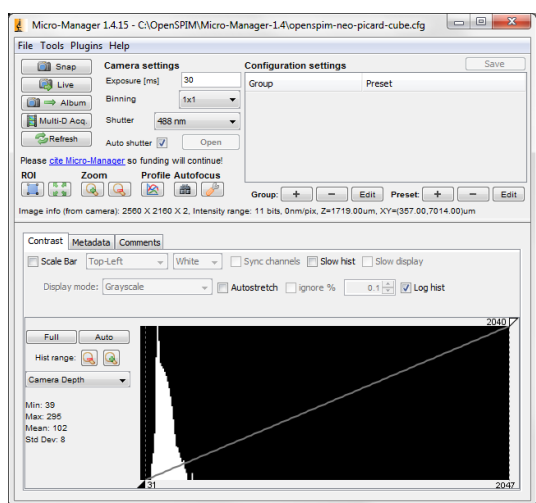


**Figure 23:** The main window of ImageJ/Fiji where all the features and plugins are made accessible.

The second is called  $\mu$ Manager (Stuurman et al. 2007); it is open source microscope acquisition software normally bundled with ImageJ. But we packaged it in such a way that we run it as a plugin in Fiji. **Figure 24** shows the main window of the program.



$\mu$ Manager had a limitation when we started using it that would only control 3 axes of motorized translation. Also the 4D motor system from Picard Industries did not have any drivers that could talk with  $\mu$ Manager, but it also had an extra dimension of rotation that needed steered via  $\mu$ Manager as well. So we hacked both: We made a plugin for  $\mu$ Manager that treated the rotation axis as another Z axis, and we tweaked the library files for each of the motors from Picard Industries 4D motor system to be able to be recognized and controlled via the plugin.

**Figure 24:** The main window of  $\mu$ Manager where all the features and exposure time of the detector can be adjusted.

The laser and camera drivers worked already very well with the software, so it was much less of an issue. Since there is a possibility for the laser to be triggered via the software as a shutter, we used this feature.

### 2.5.1 LAYOUT OF THE $\mu$ MANAGER PLUGIN

The  $\mu$ Manager plugin was designed by Johannes Schindelin and kept up to date by Luke Stuyvenberg at the Laboratory for Optical and Computational Instrumentation (LOCI) department at the University of Wisconsin at Madison. It was very much a work in progress as it was being developed; new features were added as we needed them.

There are two main tabs above called “Stage Controls” and “Acquisition”.

#### 2.5.1.1 STAGE CONTROL TAB

The first main tab is called Stage Control; it has no sub-tabs beneath it. **Figure 25** shows the window for positioning the 4D motorized stage.

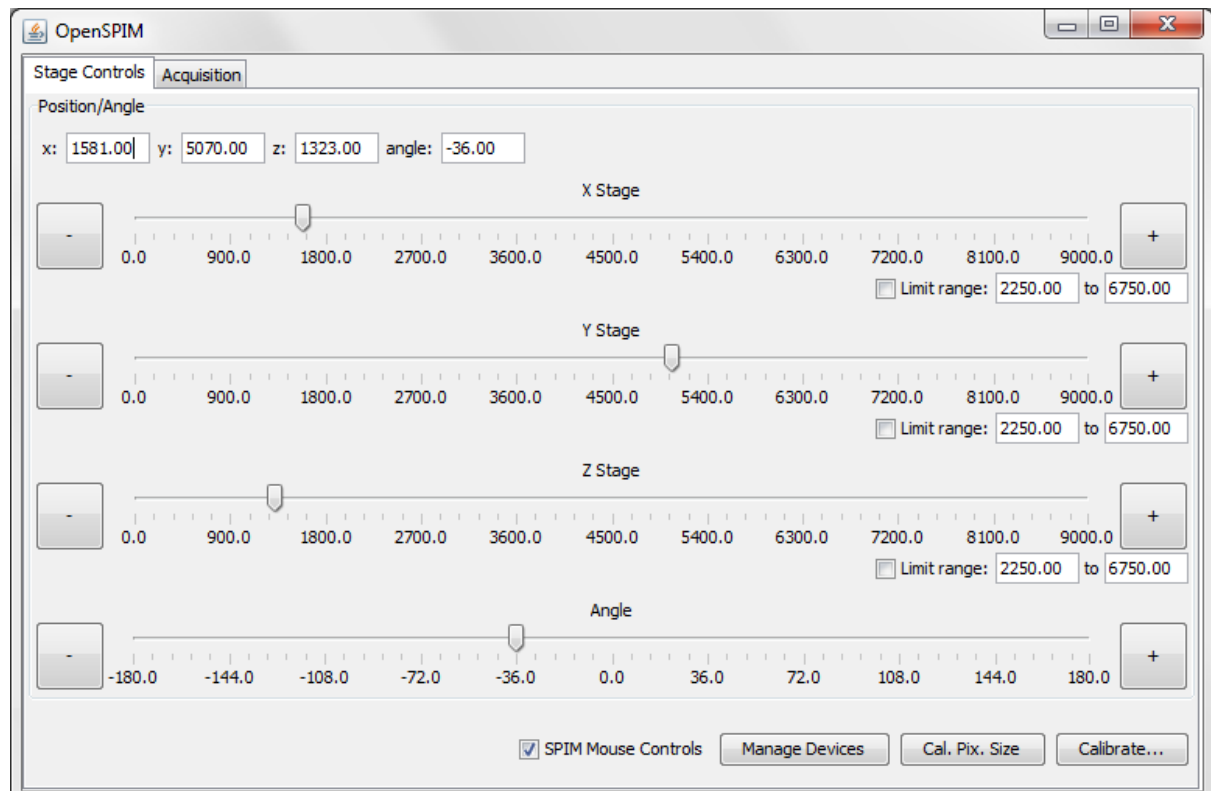


**Figure 25:** Stage Control tab window where the positions of the motors can be adjusted for imaging.

Directly under the Stage Control tab are four boxes horizontally oriented with the positions of all of the motors in relation to their respective “home” or “zero” states. One can insert a numerical text position where the respective motors should go to after pressing enter or return. Home refers to the translation motor’s fully retracted position; from there the stage travels away from where the motor is. Zero is the rotation motor’s reset.

Below the four horizontally oriented boxes are four vertically oriented horizontal scale sliders with graduated steps for the 3 translation (X, Y, & Z Stages) motors and the rotation (Angle) motor. A mouse click and drag can move the motors to where the position marker is in regards to the

graduated steps. On each side of the slider bars are buttons: a minus button on the left, and a plus button on the right. A click on either one will move the motor one position in the desired direction. If the shift key is pressed while clicking either button is clicked, the motors will move 10 positions in the desired direction. The limit range tick box along with the two insert boxes are to lessen the amount of graduated steps on the slider bar so that it doesn't jump too far with a small movement, just insert the lower number into the first box and higher number into the second.

When the SPIM Mouse Controls box on the bottom of the page is ticked, the Live window is able to be the steering point by drag and drop mouse controls. This makes life a lot easier than using only the plugin controls such as the slider. The button to the right of the SPIM Mouse Controls box is the Manage Devices button, is for making sure everything is under control in terms of hardware. The next button to the right is Calibrate Pixel Size, this is necessary to do to make sure that the motors will move correctly in the Live windows while the SPIM Mouse Controls box is ticked. And the last button in the lower right hand corner is for Calibration.

### 2.5.1.2 ACQUISITION TAB

The second main tab is called Acquisition and it has three sub-tabs: SPIM Ranges, Position List, and Video. The bottom half, as seen in **figure 26**, of each sub-tab is the same across all windows, and its settings are used throughout the functions of all three. Due to the fact that we do not use the SPIM Ranges tab in every day life, it will not be covered in this dissertation.

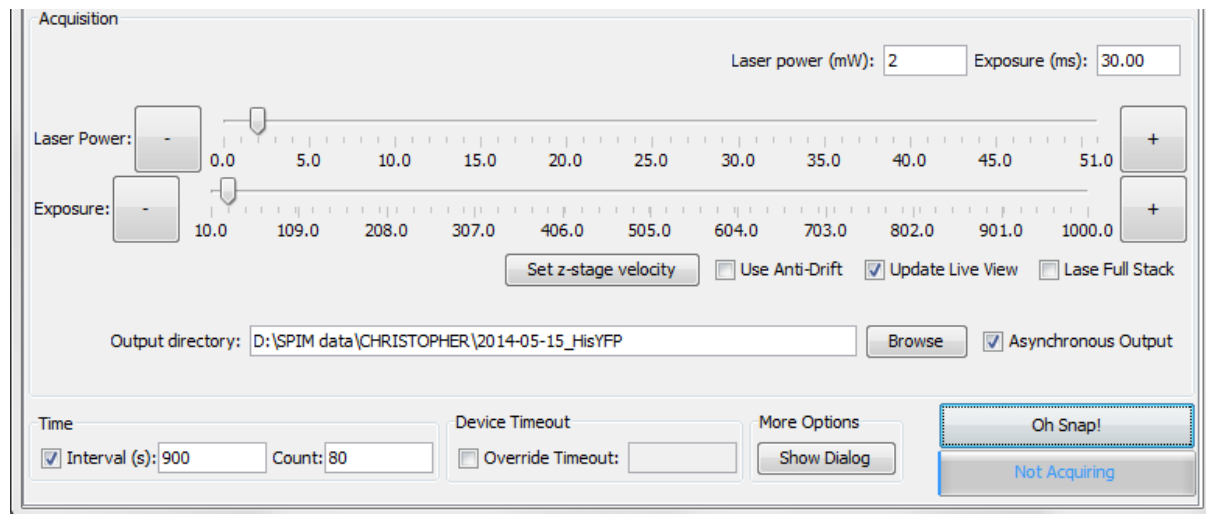


**Figure 26:** The bottom portion of the Acquisition tab window where the laser power, detector's exposure time, and output directory path can be adjusted for imaging. Time intervals and number of time points can also be adjusted here.

The Acquisition box is the upper three quarters of the lower half of the window. The two input boxes in the upper right of the bottom half let one define the laser power and acquisition time of the detector manually; the sliders right below them do this as well. The Set z-stage velocity button does exactly that, the translational motors have 12 speeds that they can be set to. But this button only affects the Z motor. The Use Anti-Drift box is a powerful tool that keeps the sample in the middle of the field of view in multi-view imaging experiments when ticked. The Update Live View box will show the progress of the Z-stack while it is being acquired when ticked. The Lase Full Stack box will not blank the laser when a Z-stack is in progress, but keep it on during the entirety of the stack acquisition. The Output directory is where the Z-stack data stored, along with a Browse

button to help you find a suitable directory or make a new one. The Asynchronous Output box implements a mode of saving data streaming from the camera to the hard disk when ticked.

In the lower left corner is a Time box, in it as a Interval tick box that measure in seconds the interval from start of the first stack or time point to the beginning of the second. The Count is the quantity of stack or time points that are to be acquired. To the left of that is the Device Timeout box an has an Override Timeout tick box and input that when ticked will give leeway to slow connections.

Finally to start the acquisition of the data is the biggest button in the whole window. The Oh Snap! Button. Below that is a status bar that shows the progress of the based on variables setup in the window.

#### 2.5.1.2.1 POSITION LIST SUB-TAB

The second sub-tab under the Acquisition tab is the most often used by our lab here in Dresden. **Figure 27** shows the window where positions can be stored for use in the acquisition.

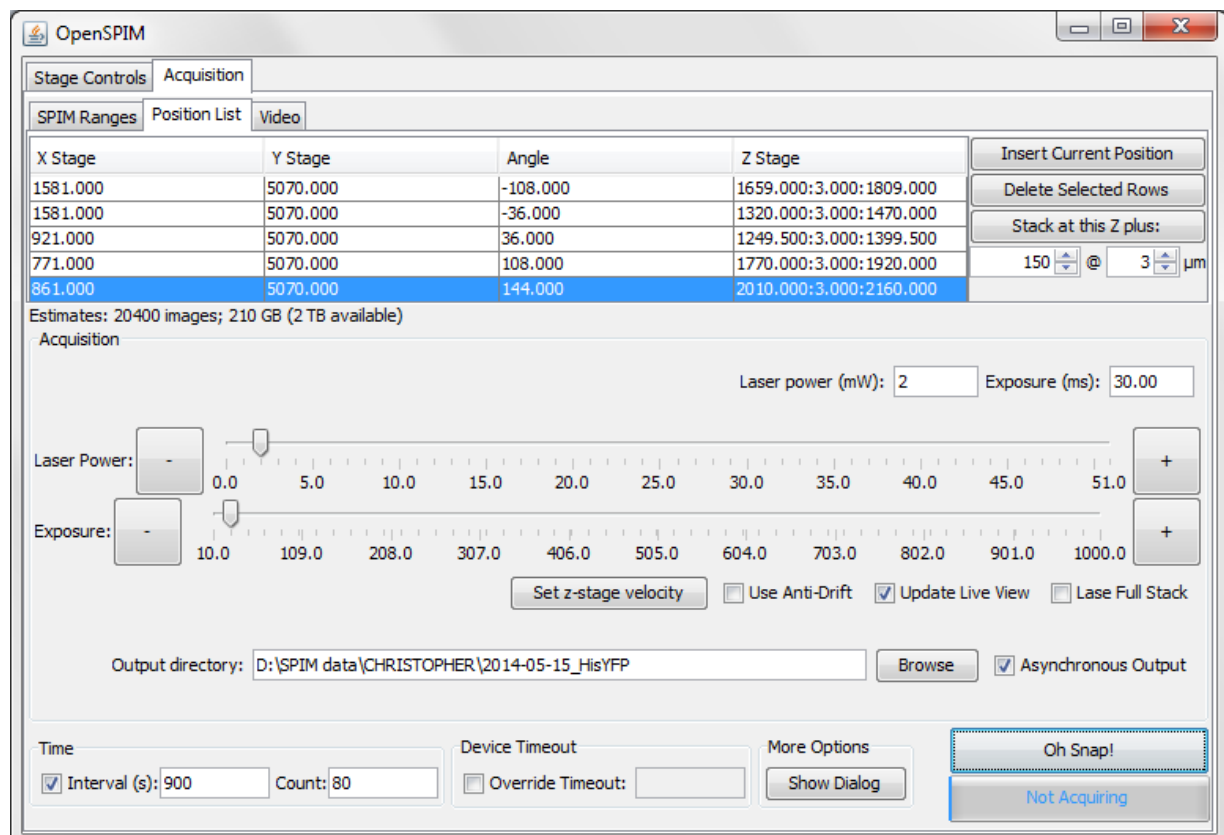


**Figure 27:** The Position List sub-tab portion of the acquisition window where a list of positions is stored for use with either large area of specimen or multi-view angles can be implemented.

This tab is in constant need of the Stage Control main tab. Using the Stage Controls; one positions the sample in the orientation that best fits the method of imaging. For example, if one were to do a multi-view or even a single-view imaging experiment the next steps described would be: With the light sheet on, position the sample in the middle where the signal is more or less fuzzy and remember the Z position. Push the sample away from the detection objective and it comes into better focus due to less scattering of the light sheet and (then around 20% further if doing multi-view

registration with beads). Note how far the sample has moved. Go back to the original position where the sample was fuzzy, and navigate to the Acquisition tab's Position List sub-tab and on the right are two input boxes with arrows on the side of them with an @ (at) sign between them. Insert the distance necessary to traverse the length travelled, and then choose the step size to be used for the Z-stack. When the numbers are inserted, click the Stack at his Z Plus button. It will insert a line in the position list with the positions that the X, Y, and Rotation motors will work at, along with the range that the Z-motor will move. In multi-view imaging, this step is repeated with different views/angles by changing the position in X, Z, and Rotation accordingly.

The position list is a comma-delimited list, which means one can select one or all of the entries and copy paste them to a text file. This makes it easier to make small changes to the positions that can be copied pasted back into the position list to be executed. One can also select one or more lines in the position list to delete them with the Delete Selected Rows button. If one clicks the Insert Current Position, then only the positions of the motors 4D stage is recorded.

#### 2.5.1.2.2 VIDEO SUB-TAB

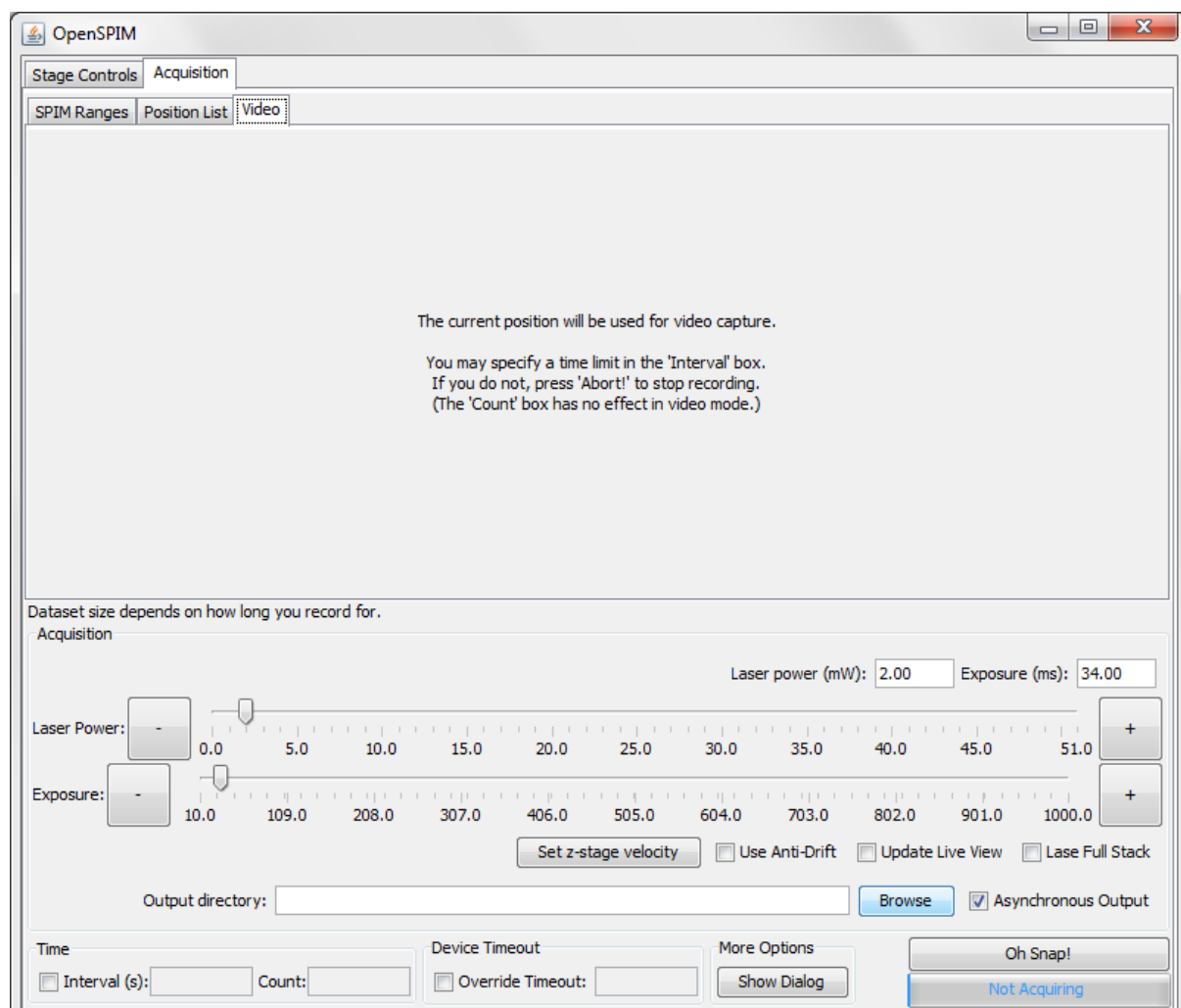


**Figure 28:** The Video sub-tab portion of the acquisition window. The only thing that can be adjusted in this window is the total time to acquire the movie and where to put the data.

The video sub-tab is by far the easiest to operate. It just uses the position that the sample is in at the time and takes as many images as the camera can stream. There is the option to make a time limited

acquisition by ticking the Interval box and inserting the time in seconds for the length of the time lapse. Otherwise to stop the acquisition, one would have to click the Oh Snap!/abort button. **Figure 28** shows the window of the sub-tab.

## 2.6 PROCESSING OF MULTI-VIEW DATA

After obtaining multi-view datasets one must register (Preibisch et al. 2010) them in relation to one another via the fiduciary markers (sub-resolution fluorescent beads) that were surrounding the sample during acquisition.

After the registration of the data, a multi-view fusion of the registered data is necessary for merging the multiple data sets into a single one (Preibisch et al. 2009). De-convolution on the datasets is possible (Preibisch et al. 2014) due to the sub-resolution beads having a PSF that can be measured.

There is really too much information to cover here in this dissertation, but it has been written about on the Fiji wiki already: [http://www.fiji.sc/SPIM\\_Bead\\_Registration](http://www.fiji.sc/SPIM_Bead_Registration), and also the OpenSPIM wiki: <http://www.openspim.org/Registration>

### 3 RESULTS

Because the OpenSPIM system is the result of this dissertation and work, I will use this section for stress tests that can help measure the stability of the system. The first sub-section will cover calculating and measuring the light sheet thickness. The second sub-section will cover measuring the PSF of the objectives, speed of the OpenSPIM system. Finally in the last sub-section a selection of imaging results will be shown.

#### 3.1 LIGHT SHEET CHARACTERISTICS

##### 3.1.1 CALCULATING THE LIGHT SHEET THICKNESS

According to Gaussian Beam Propagation the waist (thickness) of the beam at the focus point (of the illumination objective) is lambda times the focal length of the lens over Pi times the radius of the incoming beam, or: thickness =  $\lambda \cdot f / \pi r$ . Since this uses a radius instead of a diameter the real thickness is twice the answer, but we will use the calculated thickness in this section. The beam diameter filling the back aperture will make the difference in thickness; the thicker the incoming beam is the thinner the light sheet is in the focus volume.

On the other hand the calculation for the uniformity of the thickness over an extended length (diverging till it reaches the square root of two times the thickness, also known as Rayleigh length) is: length =  $\pi \cdot \text{thickness}^2 / \lambda$ . In reality this length is also doubled because we used the answer from the last calculation. Because of the phenomena of the beam diameter and thickness, one can see how when the incoming beam is larger the length of uniformity is shorter.

As can be deduced by reasoning and also the math, the differences in  $\lambda$  would create different thicknesses in the sample chamber; this is why using some form of chromatically corrected lenses for the illumination system is desirable, even achromatic lenses help in these cases.

In **figure 29** a diagram of the calculations in section 3.1.1 is shown in a graphical representation of how the light sheet would look like from above.

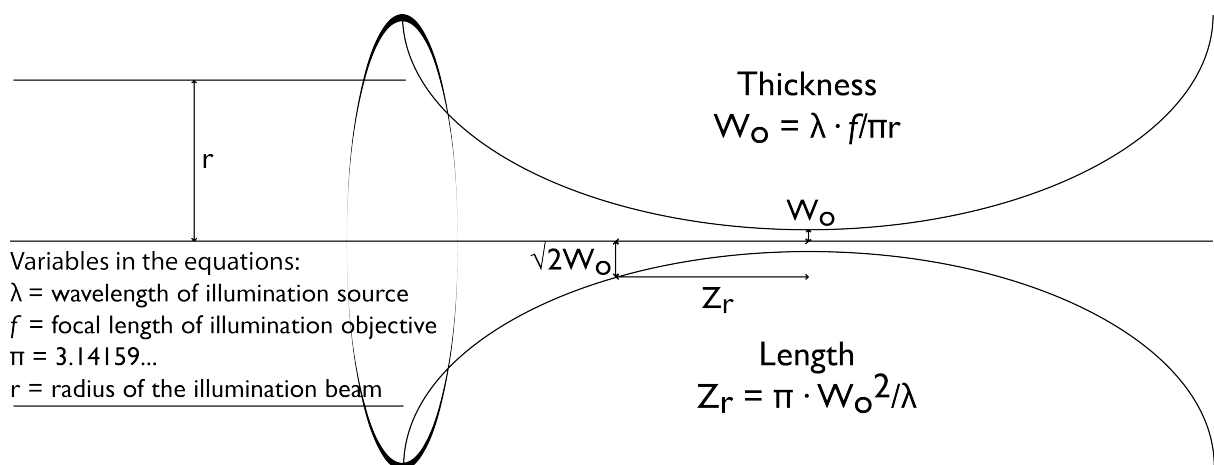


**Figure 29:** A graphical representation of how the light sheet would look like from above. The calculations are included to make the concept easier to comprehend. In table 2 both the thickness and the length are doubled because that is how it is practically measured.

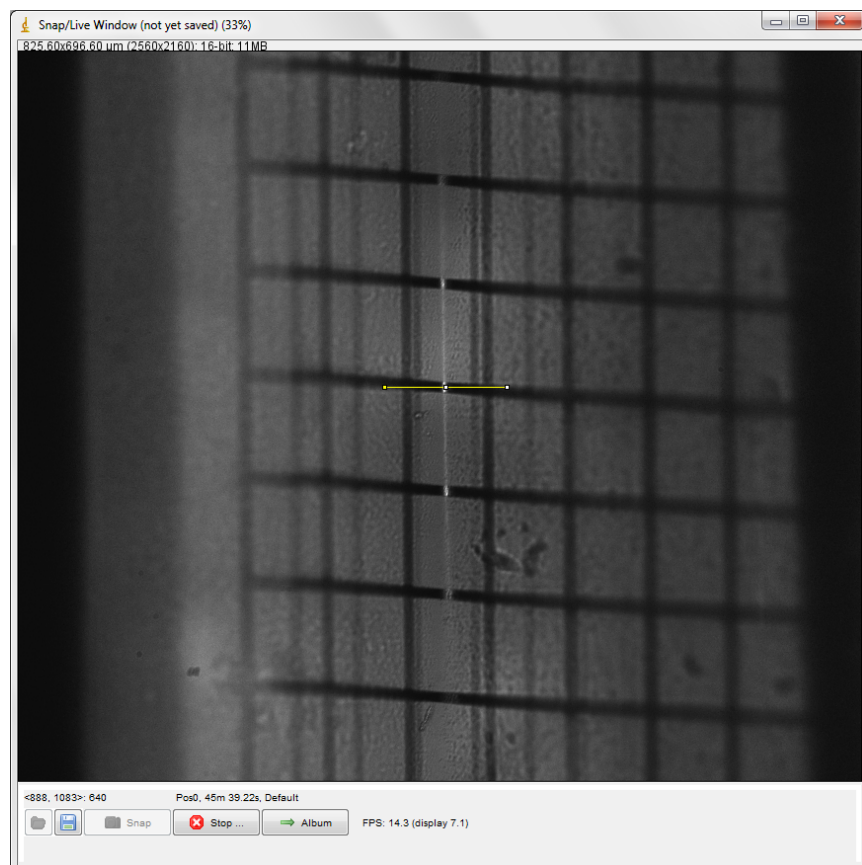
For an example, **table 2** shows three different incoming beam diameters where 488 nm is the  $\lambda$  and 18 mm is the focal length (which it is in the case of the 10x/0.3 water-dipping objective). The corrected (doubled width and length) answers are used in the table to give realistic and practical properties of the system, but keep in mind that this is only theoretical and not a perfect representation of reality:

Beam Diameter	2 mm	3 mm	4 mm
Thickness	5.59 $\mu\text{m}$	3.73 $\mu\text{m}$	2.80 $\mu\text{m}$
Length	100.71 $\mu\text{m}$	44.76 $\mu\text{m}$	25.18 $\mu\text{m}$

**Table 2:** This table shows the differences between varying the beam diameter using the same objective lens and laser wavelength (488 nm).

### 3.1.2 MEASURING THE LIGHT SHEET THICKNESS

Measuring the thickness of the light sheet can be a tricky thing to do correctly. Firstly one must know the dixel size of the detector, and the magnification factor of the detection objective. Once this is known, then figuring out the pixel size in the image is easy: use the dixel size (distance) as the divisor, and the magnification factor the number the divisor divides into. Secondly one must make sure that the exposure time of the detector does not let the laser patch to be over saturated (set it to around 3/4 to 4/5 of its full dynamic range).



Make sure the light sheet is properly aligned as discussed in section 2.3. Using the microscopy grid test sample, described in that sub-section, rotated to 45°, find a place with a reflective surface. Take an image of this and then make a line perpendicular to the patch of light as seen in **figure 30**.

**Figure 30:** An image of the microscopy grid test sample rotated to 45° with the laser light reflecting into the detector in the plane of focus of the detection objective. The yellow line is oriented perpendicular to the light sheet. A profile plot of this line will measure the thickness of the light sheet.

Next go to Analyze/Set Scale... (See **figure 31**) The window has four input boxes: Distance in pixels (preset to 0), Known distance (preset to 0), Pixel aspect ratio (preset to 1.0), and Unit of length (preset to pixel). Set the Distance in pixels to 1, then set the known distance to the calculated pixel size of the image, keep the Pixel aspect ratio, and set the Unit of length to the calculated unit of measure used (usually  $\mu\text{m}$  but sometimes light years). Make sure to tick the Global box if you want all images to be locked to this value. The information in the upper right hand corners of the open images will change according to what was entered.

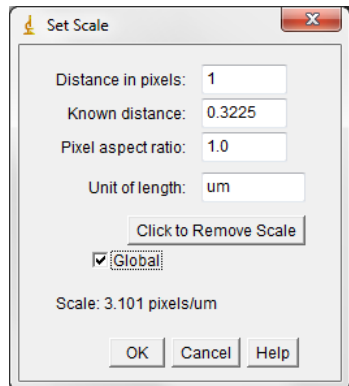


**Figure 31:** The Set Scale window

Once the scale for the images is set then the line in the image (see **figure 30**) can be plotted. **Figure 32a** shows the window with the measurements plotted, the Y-axis is intensity (which is very important to make sure that it is not clipped at the top – i.e. over saturated) and the X-axis is distance. **Figure 32b** shows a way to get a close approximation of the light sheet's thickness. Draw the same kind of line in the plot window across the middle of the peak and measure the line by going to the Fiji menu: Analyze->Measure the result will be like the Results window in the figure.

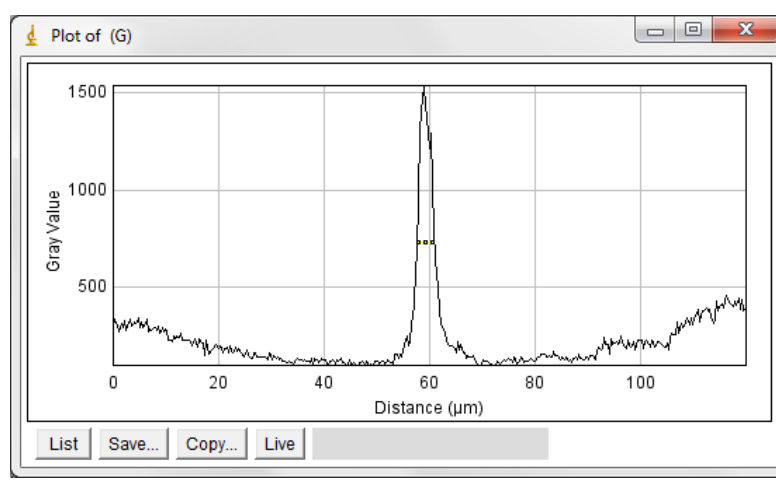
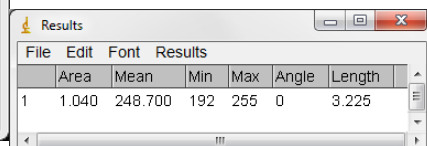


**Figure 32 a & b:** (a) The Plot of (...) window graphically showing the intensity (Y) over distance (X). along with a yellow measuring line. (b) The Results window after measuring the Full Width at Half Maxima (FWHM) by eye and steady hand, not a very accurate way to measure, but it gives a good idea the sheet's thickness.



To get better results, click the List button in the lower left hand corner to get another window (as seen in **figure 33**). This window is just the comma-delimited list of xy coordinates for the profile plot (see **figure 33a**). Scroll down to the highest Y value, this is where the laser is, take note of what it is. With the value in mind, divide it in half and find the 2 closest corresponding values on either side of the peak (or above and below in the list). The difference of these two x values is the thickness of the light sheet.

X	Y
56.7600	315.0000
57.0825	416.0000
57.4050	606.0000
57.7275	674.0000
58.0500	977.0000
58.3725	1309.0000
58.6950	1483.0000
59.0175	1538.0000
59.3400	1431.0000
59.6625	1376.0000
59.9850	1218.0000
60.3075	1299.0000
60.6300	1024.0000
60.9525	791.0000
61.2750	660.0000

**Figure 33:** The Plot Values window that shows a list of the line profile. The maximum Y value is the laser; the X value is where it is positioned in relation to the line drawn in the image. To find the Full Width at Half Maxima (FWHM), divide the Y value in half and find the two nearest X values that correspond to that value. For example in this window the position with the highest Y value is at 59.0175 at 1538, and half that value is 769. The two nearest X values with similar Y values are 57.7575 and 60.9525 which has a difference of 3.195  $\mu\text{m}$ .

Thus the theoretical value of **2.80  $\mu\text{m}$**  calculated in section 3.1.1. (**Table 2**) is a relatively good approximation of the real light sheet thickness that we measured at **3.12  $\mu\text{m}$** .

### 3.2 MEASURING THE POINT SPREAD FUNCTION OF THE OBJECTIVE

While the PSF of the illumination objective will not affect the image as much as the detection objective due to it's long stretched out focus (because the full aperture is nowhere close to being filled), the suggested test can be used for both lenses as long as they are used on the detection axis.

Take a Z-stack of 75-100 planes in of suspended fluorescent beads in a 1-2% low melting point agarose column surrounded by a medium consisting of mainly of water. Set the brightness of the Z-stack images to a setting that allow one to see the beads, as it is good practice to use less bright beads so they don not disturb the signal from the sample. Using the magnification button in Fiji (see **figure 23**), zoom into a singe bead that catches the eye as being the special kind of loner. Using the crop tool button on the same window, crop a box with the bead in the center and large enough to capture the divergence, and loss of intensity, of the light coming from the bead when scrolling through Z with the mouse wheel. Ideally the divergence and intensity loss should be equal on both sides of focus, but that's what this test is going to determine. Test how far the scroll wheel goes either side of the bead before all noticeable intensity disappears, and which planes to start and stop from. Duplicate the cropped selection (see **figure 35**) by going the way of the Name the file in the

Title: box to something meaningful (such as XY), tick Duplicate stack box, and then insert the range from where the numbers of the planes that were chosen for the start and stop of the Z-stack separated by a minus (or hyphen) sign. It will create a duplicate dataset window of just the data that was specified. While still leaving the original Z-stack open.

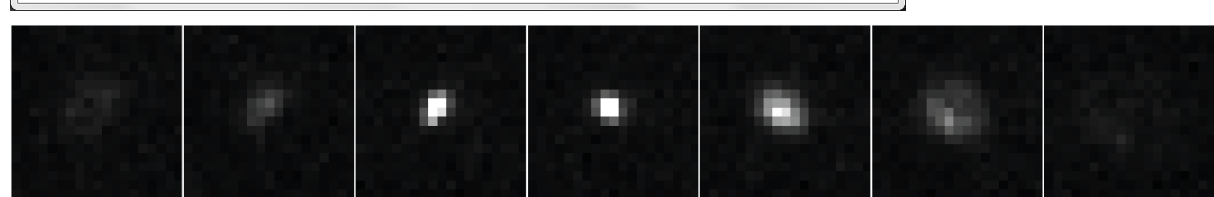
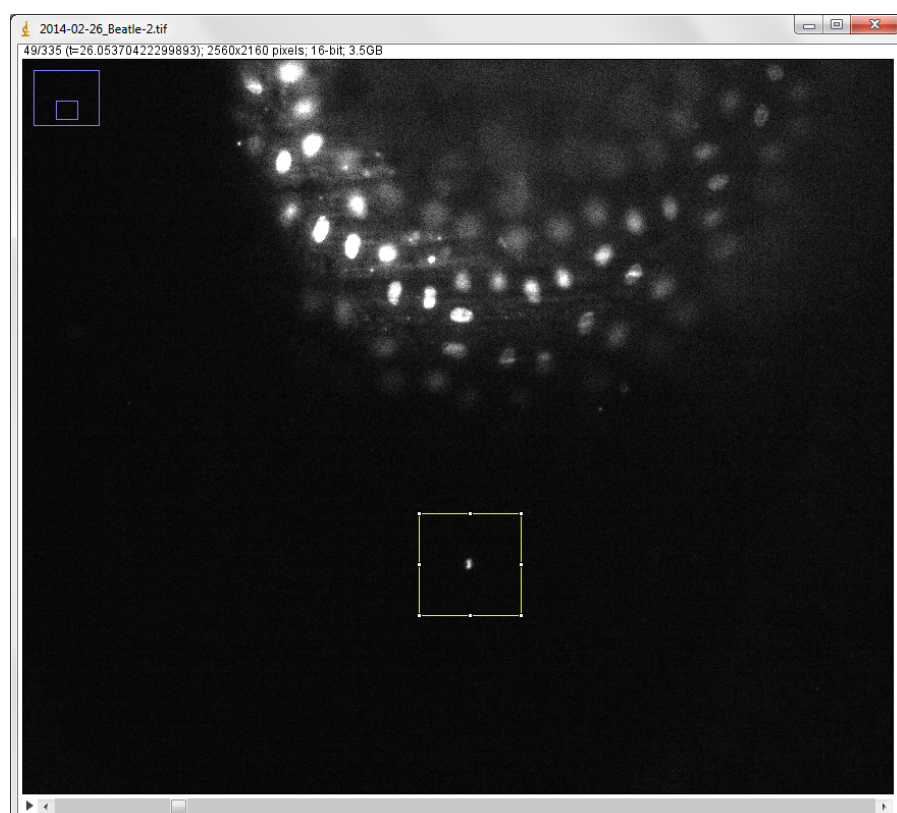
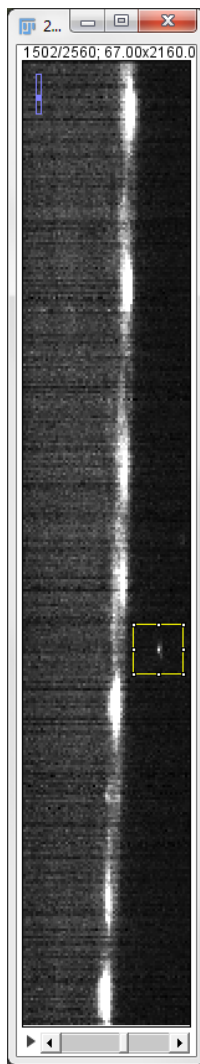


**Figure 35:** A plane by plane replay of the cropped bead through the Z-axis.



Now that the XY Z-stack is made, a stack from the original needs to be made with another viewing angle. It does not matter which axis is chosen (whether X or Y), but for sake of clarity I will choose the Y-axis for this tutorial. A rotation can be made by a plugin called TransformJ (see **figure 36**) by going to the Fiji menu: Plugins->Transform->TransformJ->TransformJ Rotate. Insert either 90° or -90° in the axis of choice. It will calculate a new stack (see **figure 37**) that looks at the sample the other axis and Z (in my case XZ). Follow the same procedure above regarding finding a single bead and setting the brightness contrast. It will be very easy to see that the shape in this axis is much different in terms of shape. Duplicate a single bead stack (see **figure 38**) like before for characterization of the PSF.

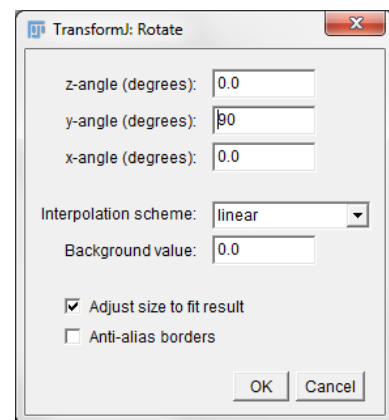


**Figure 36:** TransformJ window

**Figure 37:** Crop selection on a zoomed in Y-stack of a *Tribolium* embryo

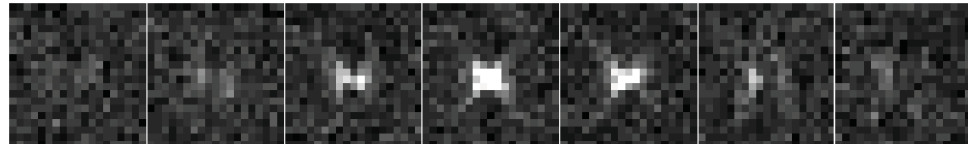


**Figure 38:** A plane by plane replay of the cropped bead through the Y-axis

### 3.3 SPEED BENCHMARKS

The speed of the system's ability to acquire data is tied to three parameters, but the weakest one of these three links can slow the whole system down:

1. The speed of the detector
2. The speed of the data transfer from the detector to the storage space
3. The speed of the motors

The following paragraphs will cover these topics in more detail.

1.) The detectors that we have used in the past have top speed limitations from 10 fps (Hamamatsu Orca ER, QImaging Retiga 4000), to 30 fps (The Imaging Source ### {TIScam}), to 100 fps (Andor Neo). But we almost never get more than 10 fps due to fluorescence signal strength (acquisition time is almost never set below 20 ms) and motor movements (see point 3), unless we are doing a 2D video acquisition that is by far the fastest. Thus the camera does not limit the acquisition speed.

2.) The speed of the data transfer off the detector to the computer is limited by the standard that is used. FireWire 800 is the standard that both the Orca ER and Retiga 4000 used, it has a data transfer rate of 800 Mbit/s. The TIScam used USB2, which has a data transfer rate of 460 Mbit/s. But

the new USB3 Standard has transfer rates of 4 Gbit/s, which will be very interesting when detectors that use this standard become more prevalent and widely used. The Neo uses Camera Link, which is capable of 6 Gbit/s. Unfortunately a special computer card is necessary for its use. These speeds are never a problem when doing Multi-view time-lapses due to the fact that anything less than 10 fps is well under the range for even USB2, so in this scenario the transfer rate does not limit the acquisition speed either.

3.) The Picard Industries 4D Motor System that was built after my initial design has 12 step rates of 0.5 ms each; starting from 6.5 ms for the slowest, and 1.0 ms for the fastest. This is both for their translation motors and their rotation motor. The rotation speed is very fast, so it does not contribute to slowing down the system in any way. During the 2D video acquisition, the motors do not move so it is extremely fast. However sample translation is the dominant factor limiting the speed of acquiring 3D multi-view datasets.

So to conclude, all of these three parameters play a role in the speed of the OpenSPIM system. But the motors are by far the slowest component of the three.

### 3.3.1 THE LASE FULL STACK OPTION FOR INCREASING SPEED

The option to Lase Full stack given in the lower portion of the Acquisition tab makes it possible to save some time in imaging due to the fact that the system does not communicate to the laser to turn itself off after every image capture. **Table 3** shows the differences in speed between single plane movies\*, a single-view Z-stack, and a multi-view time point. Each with 100 planes using the Andor Neo set to 20 ms exposure time.

	2D Single Plane Video	3D Single-view Z-Stack	4D Multi-view T-Point
Lase Full Stack Off	00:00:10 (73 frames*)	00:00:43	00:04:55
Lase Full Stack On	00:00:10 (114 frames*)	00:00:17	00:03:17

**Table 3:** This table shows the differences in speeds when Lase Full Stack is used compared to when it is not.

\* The video can only be set with a time interval, unfortunately not with the count of planes desired.

## 3.4 IMAGING RESULTS

OpenSPIM can be used to image objects that are in the 50-1,500  $\mu\text{m}$  range. This sub-section will show some of the imaging results that come from OpenSPIM. It will start at the simplest imaging modalities (2D over time) and move on to the more complex (4D).

### 3.4.1 2D SINGLE PLANE TIME-LAPSE MOVIES

With the video sub-tab one can make a time-lapse movie as fast as the camera and data transfer can stream it. In **figure 39** are 10 still frames of a Tg(cmlc2:EGFP) marked zebrafish heart beating, while in **figure 40a** the morphology is revealed due to the extra contrast given via trans-lighting of the sample as compared to pure fluorescence seen in **figure 40b**.

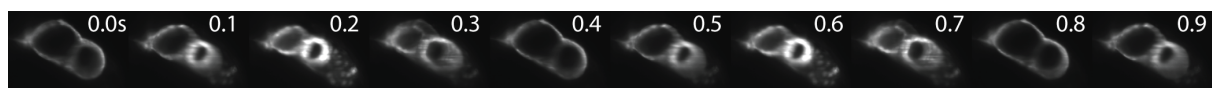


**Figure 39:** Still frames of a beating heart of 2 days old zebrafish larva expressing the cardiac myosin light chain eGFP fusion Tg(cmlc2:EGFP), serving as myocardium specific marker, was imaged with single plane illumination at 10 frames a second. Two full heartbeats are captured at this rate. The scale bar is equivalent to 100  $\mu\text{m}$ .

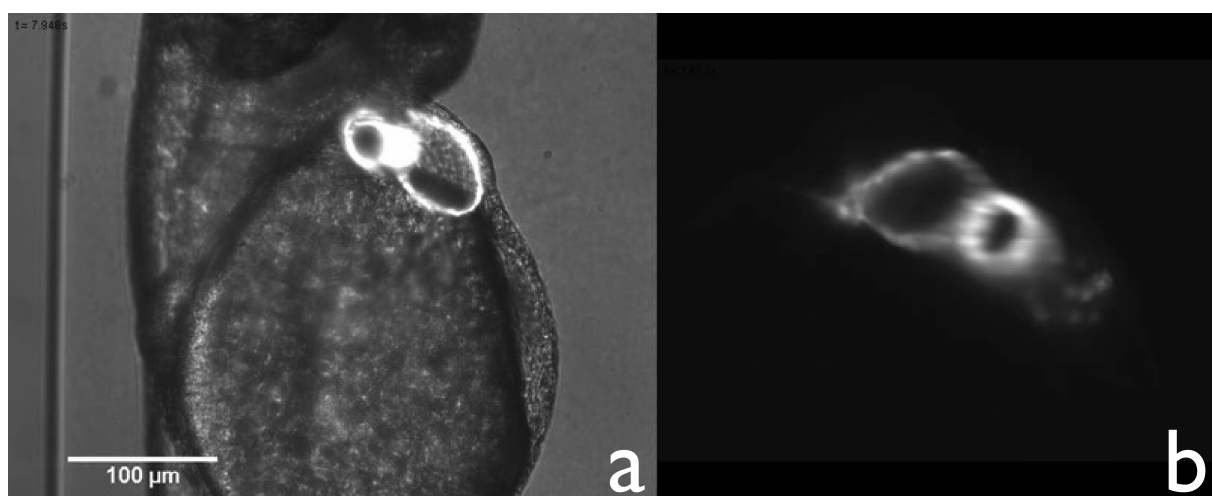


**Figure 40:** Movie of the beating heart of a 48 hpf Tg(cmlc2:EGFP) zebrafish. (a): overlay of transmitted light and fluorescence signal. (b): fluorescence signal alone, Click on the image for a supplementary video.

Thus OpenSPIM can capture even very fast biological processes such as beating heart, provided that the imaging does not require the movement of the motors.

### 3.4.2 SINGLE VIEW TILED Z-STACK OF LARGE SPECIMEN

Because of Picard Industries 4D motor system, it is possible to translate the sample in X, Y, Z, and Rotation axes. The sample in **figures 41** and **42** is a 2 day old zebrafish expressing GFP on histone molecules located in every cell nucleus, and it was imaged along its whole body axis. No rotation was made during acquisition; only the translation motors were used. The sample was primarily translated on the Y-axis and neighboring fields of view were imaged with a slight overlap (10-15%), but small adjustments to the X-axis were also done and the Z-axis was acquired at different depths. 6 tiles stacks were then acquired in the Z-axis. They then were stitched together using Fiji's native stitching plugin (Preibisch et al. 2009).

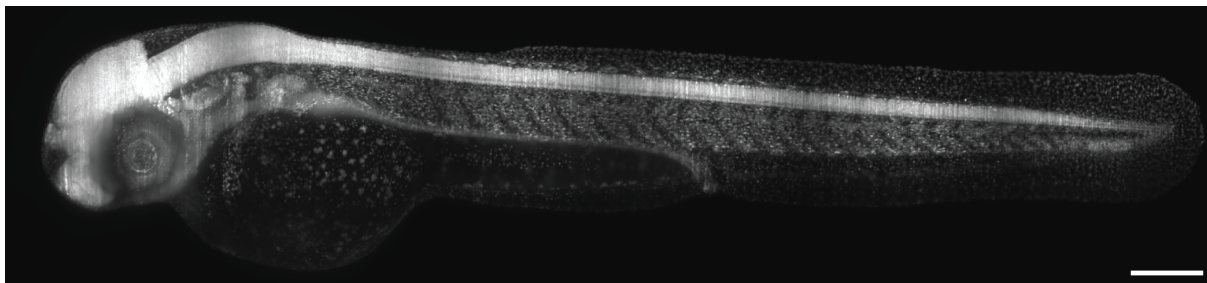


**Figure 41:** Image of a 2 days old zebrafish larva expressing H2A-GFP under the control of beta-actin promoter, Tg(Bactin:H2A-EGFP), was imaged as a set of 6 overlapping fields-of-view montaged using Fiji's stitching plugin with maximum intensity fusion method. The scale bar is equivalent to 100  $\mu$ m.

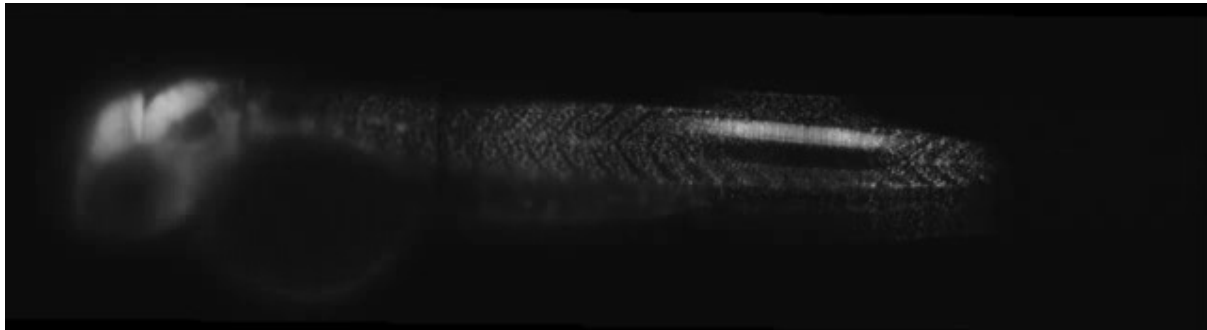


**Figure 42:** Movie of a stitched zebrafish larva. Sweep through the 3D volume of two-day-old living zebrafish larva mounted in 1% agarose expressing H2A-GFP under the control of beta-actin promoter Tg(Bactin:H2A-EGFP) in all cells imaged as a set of 6 overlapping fields-of-view of 80 slices 3  $\mu$ m apart. The stacks were montaged using Fiji's stitching plugin with maximum intensity fusion method. The scale is the same as **figure 41**. Click on the image for a supplementary video.

Thus OpenSPIM can image large static specimens in a slightly overlapping tile-wise fashion, with native Fiji plugins it is possible to stich the data together to reconstruct the whole specimen.

#### 3.4.3 MULTI-VIEW 3D IMAGING OF FIXED SPECIMEN

Using the rotation motor it is possible to acquire 3D stacks of the same specimen from different angles (views). The multi-view imaging is a unique feature of a SPIM microscope and becomes useful when imaging relatively large fixed 3D specimen such as Drosophila embryos (see **figure 30a**).

Multi-view deconvolution is a very powerful tool that can further improve the quality of the resulting 3D image. However, deconvolution has to be used carefully because it is a post-processing technique that can introduce artifacts. In OpenSPIM we use the fluorescent beads included in the agarose for registration purposes to measure the PSF of the system for the particular imaging experiment. These measured PSFs are then used for deconvolution, which is better compared to using the theoretical PSF of the system. Deconvolution is particularly useful for OpenSPIM data due to the fact that the light sheet is rather thick and thus the PSFs are rather extended in the z direction. As the deconvolution assigns photons to where they came from, it leads to substantial increase in contrast and resolution of the deconvolved multi-view data compared to data fused without deconvolution (compare **Figure 43 a and b**).

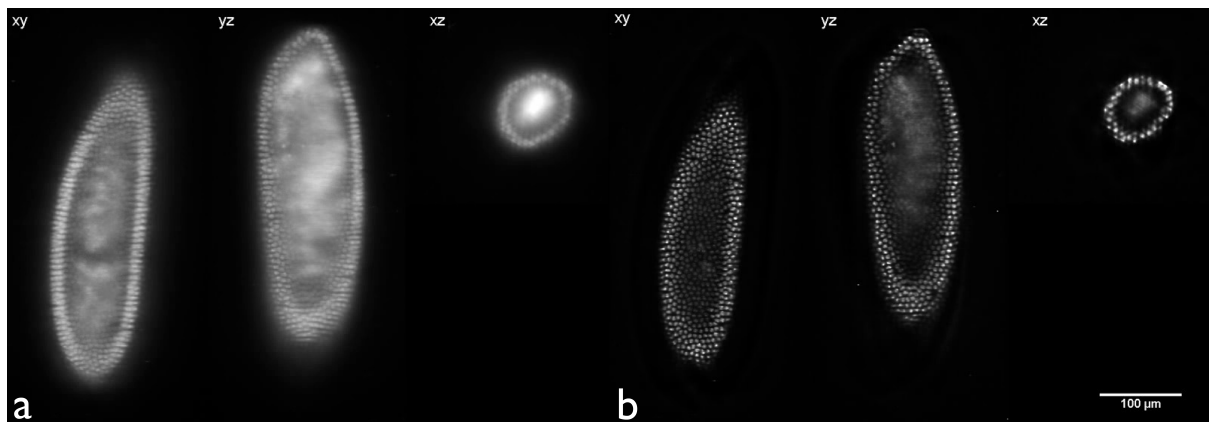


**Figure 43:** A registered and fused multi-view dataset with cross sections seen from three planes. Notice the xz plane and how it is fuzzy with very little contrast in the left side (a) compared with the one on the right (b).

Thus, with OpenSPIM one can image large fixed specimen from multiple angles and when using deconvolution to combine the data from different angles achieve image quality comparable to more sophisticated set-ups that use thinner light sheets.

#### 3.4.4 MULTI-VIEW TIME-LAPSE (4D) RECORDING OF LIVING SPECIMEN

The unique feature of SPIM in general is that it is possible to rotate the sample to acquire views that were not accessible before. With OpenSPIM it is possible to acquire multi-view datasets then register them into isotropic renderings for presentation purposes. **Figures 44, 45, 46, and 47** show two examples of transgenic *Drosophila* samples: The first two figures (**44** and **45**) are of an embryo expressing Yellow Fluorescent Protein (YFP) in the nucleus fused to the Histone molecule, and the second in **figure 46** is of an embryo expressing GFP fused to the CSP gene is expressed in the central nervous system thus marking the entire system.

**Figure 44** is a long term time lapse 4D movie of a *Drosophila* embryo expressing YFP in the nucleus of the cells imaged over 19 hours from before gastrulation until right before it hatched in the troughs of muscle contractions. **Figure 45** is a 4D movie of **figure 44**.

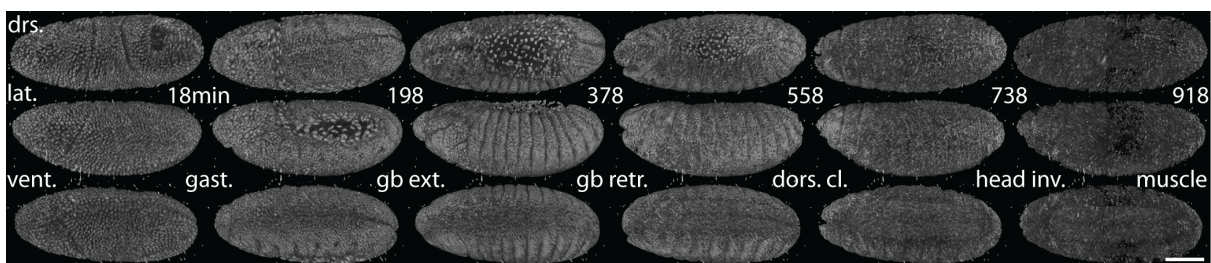


**Figure 44:** 3D rendering *Drosophila* embryos, expressing His-YFP in all cells, imaged from 5 angles every 6 minutes from gastrulation until hatching. Dorsal (dors.), lateral (lat.) and ventral (vent.) views are shown for every 30th timepoint highlighting the major morphogenetic transition in embryogenesis (gastrulation (gast.), germ band extension (gb. ext.), germ band retraction (gb. retr.), dorsal closure (dors. cl.), head involution (head inv.) and the onset of muscle contraction (muscle)).

The scale bar is equivalent to 100 μm.

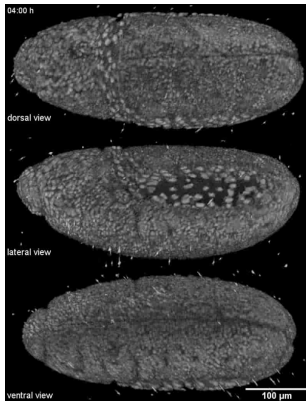


**Figure 45:** 3D movie rendering of Drosophila embryogenesis captured by OpenSPIM. Drosophila embryo expressing Histone YFP in all cells was imaged from 5 views every 6 minutes (acquisition of the 5 views took 3 minutes and 30 seconds at 1 mW laser power, 100 ms exposure time and 50 slices 6  $\mu$ m apart per view) from gastrulation until hatching. The multi-view data were reconstructed using bead based registration and fused with multi-view deconvolution for 15 iterations. A macro script exploiting Fiji's 3D Viewer was used to render the reconstructed volume from each time-point from dorsal (top), lateral (middle) and ventral (bottom) viewpoints. Note the residual beads around the sample which come from enhancement of the weak red fluorescent bead signal by the deconvolution procedure. The first 198 time-points of 235 time-point time-lapse are visualized. The scale bar is equivalent to 100  $\mu$ m. Click on the image to see the supplementary video.

**Figure 46** shows the change over time of the expression pattern of the CSP gene that is part of the central nervous system. **Figure 47** is a screenshot from a 4D movie showing the CSP expression pattern development over time.

Thus, OpenSPIM can be used to record dynamic developmental processes by multi-view *in toto* imaging.

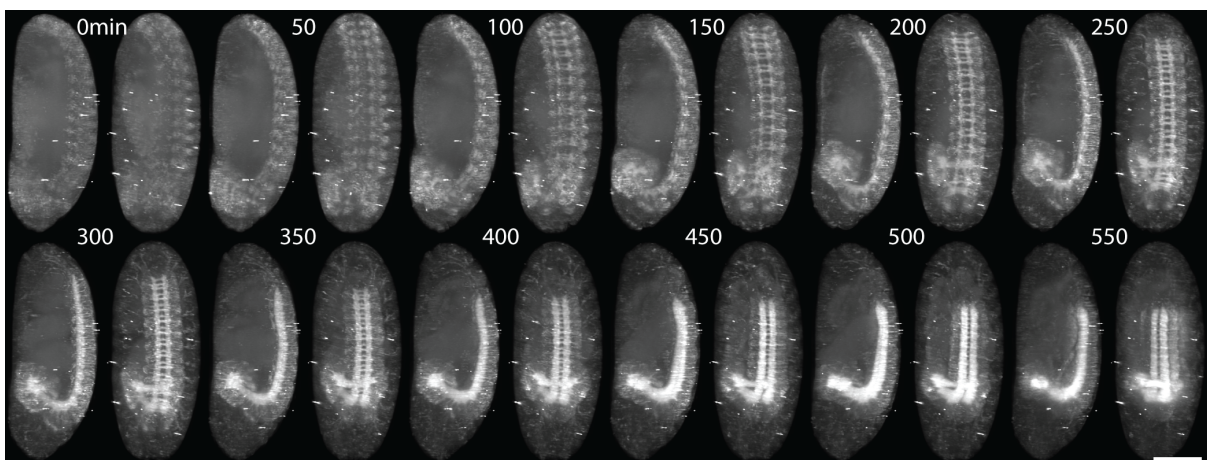


**Figure 46:** Multi-view time-lapse of the expression pattern of Csp. Drosophila embryo expressing Csp-sGFP protein fusion under native promoter control was imaged from 5 views every 10 minutes (acquisition of 5 views took 4 minutes 30 seconds at 1 mW laser power, 500 ms exposure time and 50 slices 6  $\mu$ m apart per view). On the left side maximum intensity projection along the lateral and dorsal-ventral axis are animated from germband extension stage until late embryogenesis highlighting the dynamic morphogenetic movement of the nervous system. Csp is expressed in all epidermal cells localized to the membrane and this signal dominates during earlier time-points of the movie. Over time the neuronal signal increases. The blur towards the end of the series is caused by the movement of the living embryo. The maximum intensity projection on the top right side, roughly alongside the rotation axis shows that despite the low resolution the tissue level expression pattern can be discerned. Bottom right shows 3D rendering of Csp signal over time using a fixed threshold that isolates the stronger nervous system signal revealing striking relocation of the brain hemispheres during head involution.

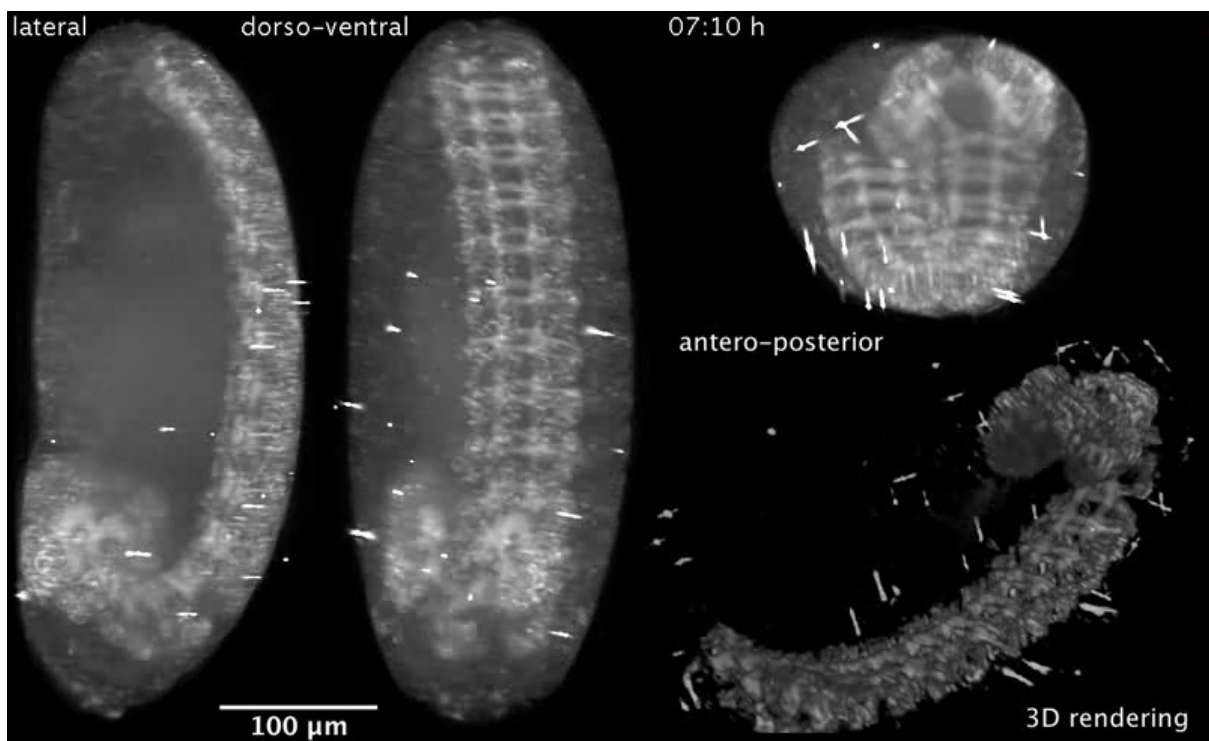


**Figure 47:** Movie of drosophila embryos expressing Csp sGFP protein fusion under native promoter control imaged from 5 views every 10 minutes. Maximum intensity projection along the lateral and dorsal-ventral axis are shown for every 5th timepoint from germband retraction stage until late embryogenesis highlighting the dynamic morphogenetic movement of the nervous system. Scale bar in all panels is 100  $\mu$ m. Click on the image to see the supplementary video.

## 4 DISCUSSION AND CONCLUSION

To conclude this dissertation a few ideas about OpenSPIM, and for its future, will be discussed.

### 4.1 AREAS WHERE OPENSPIM CAN BE USEFUL

#### 4.1.1 HIGHER THROUGHPUT - SPIM FARM



Higher throughput for less expense is one of the main reasons that Pavel Tomancak wanted to make OpenSPIM. He researches *Drosophila* genetics during embryogenesis, and how gene expression changes over that period of time. Since there are over 14,000 known genes, and his goal is to catalog their expressions, it would take more than 38 years to do with only one commercial system imaging one sample per day. Because of the modularity and relatively low price of the OpenSPIM system, it can be parallelized with multiple systems running simultaneously. **Figure 48** shows a conceptual design of four double-sided illumination single sided detection T-OpenSPIM that saves space by stacking the systems vertically on a shelf like rack.

**Figure 48:** Conceptual design of a four system OpenSPIM farm on a shelf system – Rendering by Michael Weber

#### 4.1.2 PLATFORM FOR DEVELOPMENT – OTHER CONFIGURATIONS

OpenSPIM is a very simple platform that can be expanded on in many different ways. For example, a laser ablation or cutting experiment would require only a few minor modifications to the detection beam path.

The three different common configurations developed so far for SPIM

- single sided illumination and single sided detection
- dual sided illumination and single sided detection
- dual sided illumination and dual sided detection

are all possible to build using the OpenSPIM platform (**figure 49**). We refer to them as L-OpenSPIM (**figure 49a**), T-OpenSPIM (**figure 49b**) and X-OpenSPIM (**figure 49c**). The L-OpenSPIM is the most common configuration that is already used extensively in number of labs. In the Tomancak lab we have a working prototype of T-OpenSPIM, however it is not yet fully integrated with the software. The X-OpenSPIM is an idea waiting to be realized...

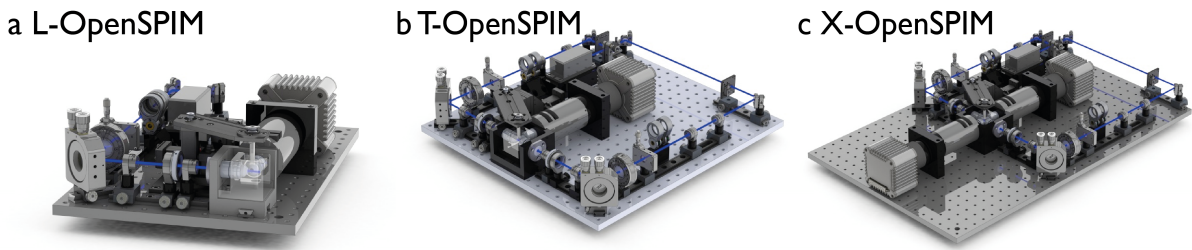


**Figure 49:** OpenSPIM configurations. (a) L-OpenSPIM with single sided illumination and single sided detection, (b) T-OpenSPIM with dual sided illumination and single sided detection and (c) X-OpenSPIM with dual sided illumination and dual sided detection.

#### 4.1.3 TEACHING TOOL

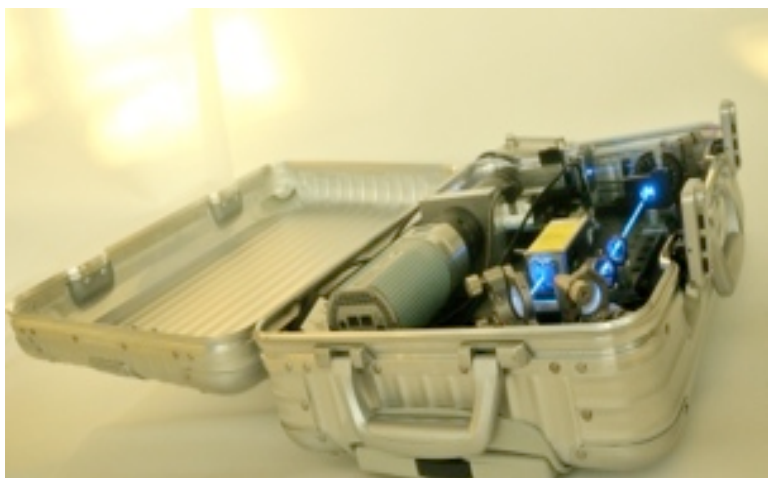
As a teaching tool, OpenSPIM can be multi faceted. Not only is it a good example of constructing an optical system, but also there are elements of electronics, programing, and biology involved.

We have taught practical courses at biological workshops where the students build the system from the components to a fully functional OpenSPIM observing living samples in just a matter of hours. **Figure 50** is a picture taken by Pavel Tomancak in Pretoria South Africa of me teaching a group of an elite high school, whose students come from across the continent of Africa, how light sheet microscopy works.



**Figure 50:** Image of Peter Gabriel Pitrone teaching concepts of light sheet microscopy – Pavel Tomancak.

#### 4.1.4 PORTABILITY – CAN BE BROUGHT TO LOCATION IN CARRY-ON



The way we brought the system to the biological workshops to teach the practical courses was in an aluminum carry-on luggage container. So far it has been to Toulouse France, Pretoria South Africa, Malmo Sweden, and Paris France. In fact in the past we used to call OpenSPIM “SPIM in a briefcase”, as seen in **figure 51**, but it sounded a little too childish for any one to take us seriously.

**Figure 51:** Image of OpenSPIM in a carry-on luggage container (“SPIM in a briefcase”) – photo by Vineeth Surendranath

#### 4.1.5 IMAGING OF VERY LONG PROCESSES

OpenSPIM can be made a work horse for the long term time lapse experiments such as observing *Parhyale hawaiesis* (crustacean) development that can take up to a full week to image. In that way OpenSPIM could supplement a commercial system in an imaging core facility where week-long experiments might be frowned upon.

### 4.2 OTHER OPENSPIM SYSTEMS BEING BUILT

As of the beginning of June 2014, Picard Industries has built and sold 42 4D motor systems (5 of them for us) with 2 new systems ordered. This gives a good idea of how many OpenSPIM systems have been, or are in the process of being, built. This gives just a rough estimate of how many OpenSPIM systems there are, because it is possible to use other manufacturers translation systems or to build one’s own 4D motor system with other components.

Picard Industries is also in the process of designing higher resolution translation and rotation stages, and will incorporate these into a new Hi-Res 4D system. They claim that the translation stages travel 0.25  $\mu\text{m}$ , and the rotation motor takes 1° steps. This is a step forward in higher resolution imaging.

I designed a Nikon detection objective chamber with a 16x/0.8 (see **figure 52**) for Carsten Wolff at the Humboldt University in Berlin for his research on evolutionary developmental biology. He came down to Dresden and we built it in a day. He also is one of the 42 customers of Picard Industries.

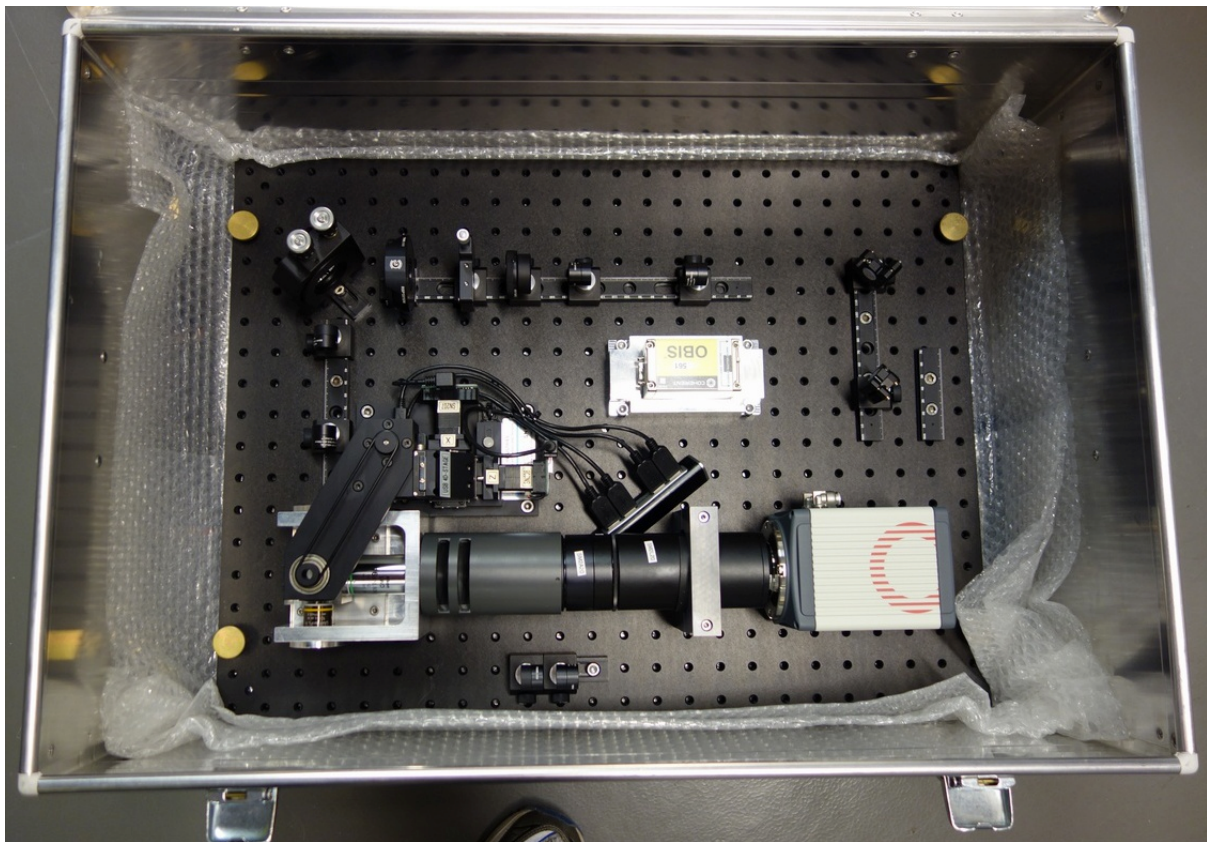


**Figure 52:** Image of Carsten Wolff's OpenSPIM system.

A list of more OpenSPIM systems that have been built that can be found on our wiki site: [http://openspim.org/Who\\_has\\_an\\_OpenSPIM%3F](http://openspim.org/Who_has_an_OpenSPIM%3F)

### 4.3 WHAT DOES THE FUTURE HOLD?

An interesting question some people ask is: what happens next? The next sub-sections will cover some ideas that I have, and components that can be implemented, to add to the functionality of the OpenSPIM platform.

#### 4.3.1 FURTHER EXPANSION INTO OTHER OPTICAL TECHNOLOGIES

Other imaging modalities can be very easily implemented in to OpenSPIM. We are already experimenting with double sided illumination and two color imaging. By pivoting the light sheet in the middle of the field of view with a single axis galvanometer scanner in the illumination beam path, one can wash out stripes caused by shadows in conventional (static light sheet) SPIM (mSPIM – Huisken et al. 2007).

OPT seems like an interesting method to implement and merge into the OpenSPIM platform, even though open access systems have already been built. (Gualda et al. 2013 & Wong et al. 2013).

Other light sheet techniques can be implemented into the OpenSPIM plugin, such as DSLM that allows for Structured Illumination Microscopy to be calculated very easily.

Another idea that I have for orthogonal microscopy is to use conventional contrasting techniques to add a layer of morphological information to the selectivity of light sheet fluorescence microscopy.

But this must be done on either a T-OpenSPIM or X-OpenSPIM due to the fact that it would require juxtaposed objective configurations to be done properly.

---

#### 4.3.2 WHITE LIGHT LASERS

Recently there have been great strides in the laser technology sector, the production of fiber optic cables with special inner cores have made it possible to create a broad spectrum of light across the visible range far into the near infrared range (450-2,600 nm). This can be amazingly useful for LSFM due to the fact that an excitation filter wheel could be used to selectively choose certain bandwidths while blocking the rest very well. With a single or double 6-position filter wheel one could do 3-4 color imaging with out much trouble in a relatively short amount of time.

A multi-band (triple or quadruple) emission filter would be used in the infinity space between the detection objective and the tube lens, it would have to match the single band pass excitation filters that would be installed in the filter wheel for the multi color experiment. If a double wheel is used then the second wheel could be filled with neutral density filters to attenuate the light intensity.

The white light laser is not a cheap option (35-45k EUR), but it could be an economical one when considering that individual laser lines can cost 5-10k EUR.

---

#### 4.3.3 FURTHER COST REDUCTIONS TO OPENSPIM COMPONENTS

3 things that cost the most in building an OpenSPIM system are: the camera, the laser, and the motors. There are ways to cut the price of each of these systems down to make the OpenSPIM system more affordable to high-schools and universities that do not have sufficient funding for a more expensive system.

By using consumer grade equipment such as mirror-less interchangeable lens cameras that are now out on the market, it is possible to spend an order of magnitude less money on the detector. This would be a very useful and interesting thing to implement, due to the fact that one could take the system out into the field with out the need for large power supplies that scientific grade cameras are known for. Also the camera can be detached from the system and used in the field with a lens for macro photography of the sample before ever putting it in the OpenSPIM chamber.

If specific laser lines are of little importance to the experiment at hand (i.e. if the specimen will be stained with a fluorescent dye, instead of already being transgenic), then cheaper diode lasers can be purchased to better match the dyes being used. Chinese laser companies such as Wicked Lasers (<http://www.wickedlasers.com/>) and Dragon Lasers (<http://www.dragonlasers.com/>) can be used instead.

Although Picard Industries' 4D motor system is inexpensive compared to other companies' motors, it is possible to built your own using off the shelf components. OpenSpinMicroscopy's (also known as OPenT) setup (<https://sites.google.com/site/openspinmicroscopy/> Gualda et al. 2013) uses a homebuilt system such as this; it costs far less than 1k EUR.

## 5 APPENDIX

### 5.1 LIST OF REFERENCES

- Rusk, N (2009) Milestone 4 (1911, 1929, 1967) First fluorescence microscope, First epifluorescence microscope, The dichroic mirror Nature Milestones: Light microscopy
- Siedentopf, HFW & Zsigmondy, RA (1903) Über Sichtbarmachung und Größenbestimmung ultramikroskopischer Teilchen, mit besonderer Anwendung auf Goldrubiingläser Ann. Phys. (Leipzig) Ser. 4 vol 10: 1-39
- Mappes, T et al. (2012) The invention of immersion ultramicroscopy in 1912 – the birth of nanotechnology? Angew. Chem. Int. Ed. 51/45: 11208–11212
- Voie, AH et al. (1993) Orthogonal-plane fluorescence optical sectioning: three-dimensional imaging of macroscopic biological specimens Journal of Microscopy 170/3: 229-236
- Huisken, J et al. (2004) Optical sectioning deep inside live embryos by selective plane illumination microscopy Science 305 (5686): 1007-1009
- Dink, W et al. (1999) Two-photon laser scanning fluorescence microscopy. Science Vol. 248 no. 4951 pp. 73-76 DOI: 10.1126/science.2321027
- Amos, WB & White, JG (2003) How the confocal laser scanning microscope entered biological research. Biol. Cell 95/6: 335-342
- Wilson, T et al. (1996) Confocal microscopy by aperture correlation. Optics Letters 21: 1879-1881.
- Sharp, J et al. (2002) Optical Projection Tomography as a Tool for 3D Microscopy and Gene Expression Studies. Science Vol. 296 no. 5567 pp. 541-545 DOI: 10.1126/science.1068206
- Preibisch, S et al. (2010) Software for bead-based registration of selective plane illumination microscopy data Nature Methods 7/6: 418-419
- Preibisch, S et al. (2014) Efficient Bayesian based multiview deconvolution. Nature Methods 11, 645–648 doi:10.1038/nmeth.2929
- Schindelin, J et al. (2012) Fiji: an open-source platform for biological-image analysis Nature Methods 9/7: 676-682
- Stuurman, N et al. (2007) μManager: Open Source software for light microscope imaging. Microscopy Today 15/3: 42-43
- Gualda EJ, et al. (2013) OpenSpinMicroscopy: an open-source integrated microscopy platform. Nature Methods 10: 599–600 doi:10.1038/nmeth.2508
- Wong, MD et al. (2013) Design and Implementation of a Custom Built Optical Projection Tomography System PLoS ONE 8/9: e73491. doi:10.1371/journal.pone.0073491

### 5.2 LIST OF WEBSITE LINKS

OpenSPIM Wiki	<a href="http://www.openspim.org">http://www.openspim.org</a>
Fiji website	<a href="http://www.fiji.sc">http://www.fiji.sc</a>
μManager website	<a href="http://www.micro-manager.org">http://www.micro-manager.org</a>
OPenT Website	<a href="https://sites.google.com/site/openspinmicroscopy">https://sites.google.com/site/openspinmicroscopy</a>
Picard Industries website	<a href="http://www.picard-industries.com">http://www.picard-industries.com</a>

### 5.3 ACKNOWLEDGEMENTS

I would like to acknowledge the Royal Microscopy Society for offering qualifications to people in the microscopy field; this gives us a great opportunity for further education.

Pavel Tomancak was the inspiration for the project, and I am grateful that he gave the chance to work for him. His lab is a great place to work, as anyone who has worked with him knows.

Jan Huisken and people in his lab were a great source of knowledge for me during the beginning stages of development of the OpenSPIM. The design of the system is based on Jan's original layout.

Johannes Schindelin was a major part of the project in terms of getting the software to communicate with the hardware. Without him OpenSPIM would be an expensive paperweight.

Luke Stuyvenberg is also a gifted programmer who helped Johannes and I get a lot more stuff done.

Kevin Eliceri is the director of LOCI in Madison Wisconsin and the employer of both Johannes and Luke, with out his interest in OpenSPIM neither Johannes nor Luke would be working on this project.

Ulrik Guenther is a new PhD student in our lab taking Luke's place in this endeavor, so I would like to acknowledge him as well.

Jan Peychl and the Light Microscopy Facility were very helpful in lending pieces and parts to me during construction. Jan also helped to proof read this document before submission.

Jeremy Sanderson was a very helpful and insightful mentor during the project; he even took time out of his busy schedule to help me kick start the writing and gave ideas for revising of this document.

The PhD group that helped us seed the wiki during a course was comprised of: Sonal, Suhkdeep, and Martin. Vineeth Surendranath took the artistic photographs for the duration of the course.

Other people I would like to acknowledge by name are: Florian Fahrbach, Andrea Bossi, Michael Weber, Stephan Preibisch, Loic Royer, and Jan Krieger for help with the OpenSPIM system in general, and Mark Brislin for his layperson and mother tongue views on the text of this dissertation.